Quaternary Research (2022), **109**, 83–101
doi:10.1017/qua.2021.76

Research Article

A late-glacial lake-effect climate regime and abundant tamarack in the Great Lakes Region, North America

Carol B. Griggs[a]*, C.F. Michael Lewis[b] and David A. Kristovich[c]

[a]Cornell Tree-Ring Laboratory, B48 Goldwin Smith Hall, Ithaca, New York 14853, USA; [b]Geological Survey of Canada (Atlantic), 1 Challenger Drive, Dartmouth, Nova Scotia B2Y 4A2, Canada and [c]Illinois State Water Survey, Prairie Research Institute, University of Illinois, 2204 Griffith Drive, Champaign, Illinois 61820, USA

Abstract

A unique regional climate progression, ca 14.2–11.5 cal ka BP, in the eastern Great Lakes region of North America is suggested by subfossil logs, high-resolution ^{14}C dates, and established proxy records in New York, USA. The progression began with a northern boreal-type climate ca. 14.2–13.1 ka coeval with the expansion of Lake Iroquois, a transition to a southern boreal-type climate ~13.1–12.9 ka that coincided with the transition of Lake Iroquois into progressively lower lake levels, and a continuation of the southern boreal-type climate ~12.9–11.5 ka. These conditions and changes are evident in the tree rings and relative dominance of tamarack (*Larix laricina*) and spruce species (*Picea* spp.) plus the presence of black ash (*Fraxinus nigra*) as the only thermophilous species. Together they suggest variations in atmospheric moisture levels, surface winds, temperature extremes, and/or an enhanced seasonality over time. Here we propose that the evolution of the glacial Great Lakes and their interactions with ice sheets, meltwater, winds, and regional topography created a regional glacial lake-effect climate, 14.2–11.5 cal ka BP, that was opposite to the established warming Bølling-Allerød–cold Younger Dryas climate progression.

Keywords: Glacial lake-effect climate, Younger Dryas, Tamarack, Great Lakes, Laurentide Ice Sheet, Meltwater distribution, Glacial anticyclonic winds, Prevailing westerlies

(Received 11 December 2020; accepted 29 December 2021)

INTRODUCTION

Varying climate conditions are recognized for the late-glacial (LG) interval across northeastern North America, but their regional expression remains relatively unknown. Proxy records from areas in and adjacent to the Great Lakes region suggest significant spatial and/or temporal differences in climate that result in a wide range of interpretations, many of which are still under debate (e.g., Edwards et al., 1985; Fritz et al., 1987; Shane, 1987; Tinkler and Pengelly, 1994; Yu, 2000; Yu and Wright, 2001; Laub, 2003b; Miller and Futyma, 2003; Webb et al., 2003; Gonzales and Grimm, 2009; Renssen et al., 2018; Watson et al., 2018; Fastovich et al., 2020; Renssen, 2020; Young et al., 2020).

The established climate progression of the warming Bølling-Allerød – cold Younger Dryas – warm Early Holocene (BA-YD-EH) and its spatial extent came from evidence of climate change in the Greenland ice cores (e.g., Alley, 2000, 2004) and coeval changes in other proxy records from in and around the North Atlantic Ocean and beyond (e.g., Jacobson et al., 1987; Peteet, 1995; Shuman et al., 2002; Dyke, 2005; Broecker, 2006; Williams and Shuman, 2008; Renssen et al., 2018; Renssen, 2020). However, the timing of changes in many of the proxies, especially for changes in the YD interval, is often based on the circular reasoning that changes similar to those in the Greenland ice cores were coeval rather than based on independent dates or on changes in better-dated proxy records in closer proximity to their respective sites (e.g., Miller and Gingerich, 2013; Muschitiello and Wohlfarth, 2015; Watson et al., 2018; Fastovich et al., 2020). Connection of records from the Great Lakes with the Greenland record requires independent dating due to distances, differences between continental and oceanic climates, and the possible effects of regional-scale factors.

Subfossil pollen assemblages of primarily spruce (*Picea* spp.), pine (*Pinus* spp.), and several non-arboreal species are established proxies of LG boreal climates in northeastern North America (e.g., Bartlein et al., 1986; Jacobson et al., 1987; Webb et al., 2003). Tamarack (*Larix laricina*) is not a key proxy due to its minimal pollen representation (e.g., Davis, 1969; Birks, 2003) but is often abundant in macrofossil collections (e.g., Shane, 1987; Jackson et al., 1997). Tamarack is a pioneer species and tolerant to climate extremes more than spruce (Burns and Honkala, 1990), and these two features may add to current interpretations of climate change.

In this study, climate changes evident in the tree-ring widths of 55 subfossil logs from five sites in New York, USA, are shown to be significantly different from the BA-YD climate progression (Fig. 1) and coeval with hydrologic changes in the glacial Great Lakes (e.g., Lewis et al., 2008, 2012; Lewis and Anderson, 2019). These findings suggest that the lakes were primary factors in regional climate dynamics and created a unique glacial lake-effect

*Corresponding author at: Cornell Tree-Ring Laboratory, B48 Goldwin Smith Hall, Ithaca, NY 14853, USA. E-mail address: cbg4@cornell.edu

Cite this article: Griggs CB, Lewis CFM, Kristovich DA (2022). A late-glacial lake-effect climate regime and abundant tamarack in the Great Lakes Region, North America. *Quaternary Research* **109**, 83–101. https://doi.org/10.1017/qua.2021.76

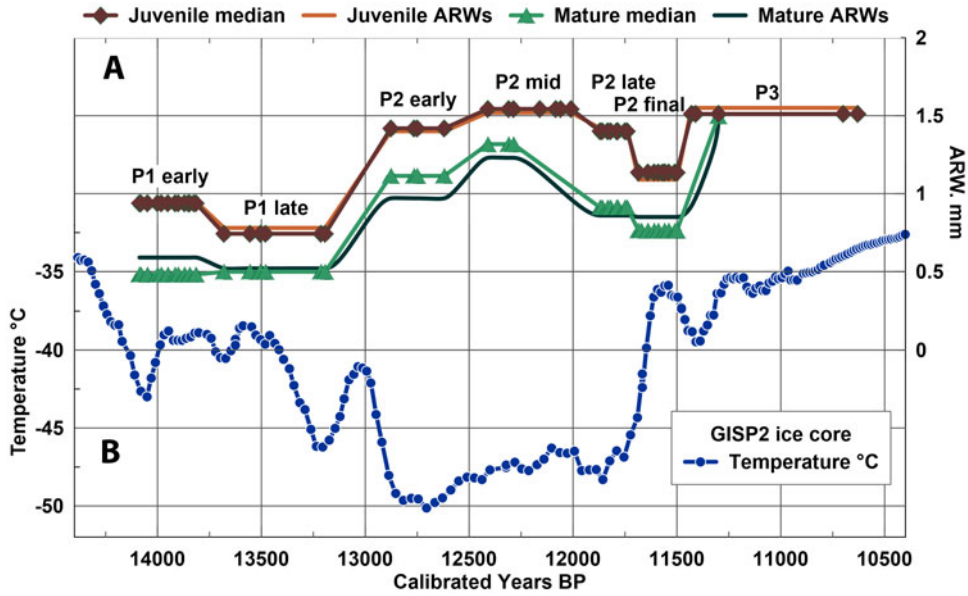

Figure 1. (A) The overall increase in tree-ring widths during the late-glacial (LG) interval, first noted in the field and later confirmed by average ring widths (ARWs); (B) the Bølling-Allerød–cold Younger Dryas–warm Early Holocene (BA-YD-EH) temperature from the Greenland GISP2 ice core (Alley, 2004). A regional climate anomaly is clearly apparent from the near inverse relationship between the tree-ring records and temperature reconstruction from the ice core data. In A, the juvenile rings are rings 1–35 and mature rings are rings 36–85 in each sample; the mean and median ARW values are used in *t*-tests and box-and-whisker diagrams, respectively. Phases P1early to P3 were identified by a clustering of the samples' calibrated ^{14}C dates over time and by differences in ARWs from phase to phase (Table 1).

climate (GLEC) ~14.2 to 11.5 cal ka BP. Here we present a working hypothesis of this phenomenon.

Background

The present Great Lakes region comprises five lakes, all of which rank in the top 12 of the largest freshwater lakes in the world and have a combined surface area of ~245,000 km^2. The lakes have mesoscale influence on climate above and around the lakes, particularly on their downwind sides (Scott and Huff, 1996; Villani et al., 2017). The geography of the study region across New York State consists of the low-relief Erie–Ontario lowlands (EOL), including the Mohawk River valley, and the higher terrain of the northeastern Allegheny Plateau (AP) (Fig. 2), a region that has been on the downwind side of lakes since deglaciation. The topography of the EOL-AP is more variable east and north of the study region, with lower relief to the west across the lakes and interior lowlands.

Between 14.2 and 10.5 cal ka BP, the glacial Great Lakes evolved from separate proglacial lakes in individual lake basins to an extensive glacial lake system, including the Great Lakes, Lake Agassiz, and the Lake Champlain basin, then back to separate lake basins with highly variable meltwater flow and no meltwater input anywhere near the EOL-AP (e.g., Lewis et al., 2007, 2008, 2012; Anderson and Lewis, 2012; Lewis and Anderson, 2017, 2019; Fig. 3). The southern margin of the Laurentide Ice Sheet (LIS) was predominantly moving northward within the Great Lakes region during the study interval, with a pause in its movement north of the Lake Huron and Lake Ontario basins ca 12.8–12.1 ka and a southward movement of the Marquette Readvance in the Lake Superior basin ca 12.5–11.5 ka (Dyke et al., 2003; Lowell et al., 2009; Rayburn et al., 2011; Lewis and Anderson, 2017, 2019; Dalton et al., 2020; Fig. 3C and D). The LIS added to the topography within the lakes region, and its relatively stationary glacial anticyclonic circulation produced strong easterly surface winds south of the LIS, forcing the prevailing westerlies to the south (e.g., Rind, 1987; Schaetzl et al., 2016; Conroy et al., 2019; Figs. 3 and 4). The westerlies likely evolved from the westerlies accompanying cold Pacific air masses to northwesterlies associated with polar dry air masses (e.g., Bryson, 1966; Rind, 1987) and altered the incoming surface winds in the Great Lakes region (Fig. 4). In addition to all these changes, the changes in the lakes' effects on weather patterns need to be considered as a viable factor in climate change but have been only occasionally considered (e.g., Saarnisto, 1974; Shane, 1987; Shane and Anderson 1993). In the next section, we summarize current lake-effect features and consider the hydrologic processes of lakes in their interactions with meltwater, ice sheets, atmospheric circulation, and topography.

Lake-effect climate dynamics

Lake-effect storms are the ultimate manifestation of a lake's influence on climate (e.g., Passerelli and Braham, 1981; Scott and Huff, 1996; Laird et al., 2003; Long et al., 2007; Vavrus et al., 2012; Villani et al., 2017), but in addition to the storms, every large lake continuously affects mesoscale atmospheric circulation, surface air temperature and moisture content, and surface winds above and around the lake, especially on its downwind side (Sousounis and Fritsch, 1994; Scott and Huff, 1996). A lake's spatial impact depends on factors such as lake size, fetch, ice-over versus open-water status, wind speed and direction, atmospheric stability, and regional topography, and extends farthest across low-relief topography on its downwind side (e.g., Libicki and Bedford, 1990; Kristovich and Laird, 1998; Samuelsson and Tjernström, 2001; Desai et al., 2009; Vavrus et al., 2012; Veels and Steenburgh, 2015; Lang et al., 2018). Multiple lakes in close proximity increase the extent and strength of impact, and the greatest impact of lake effect from the Great Lakes today is up to 300 km downwind of Lakes Ontario and Erie across most of central New York, due to prevailing westerlies, the two lakes' east-

https://doi.org/10.1017/qua.2021.76 Published online by Cambridge University Press

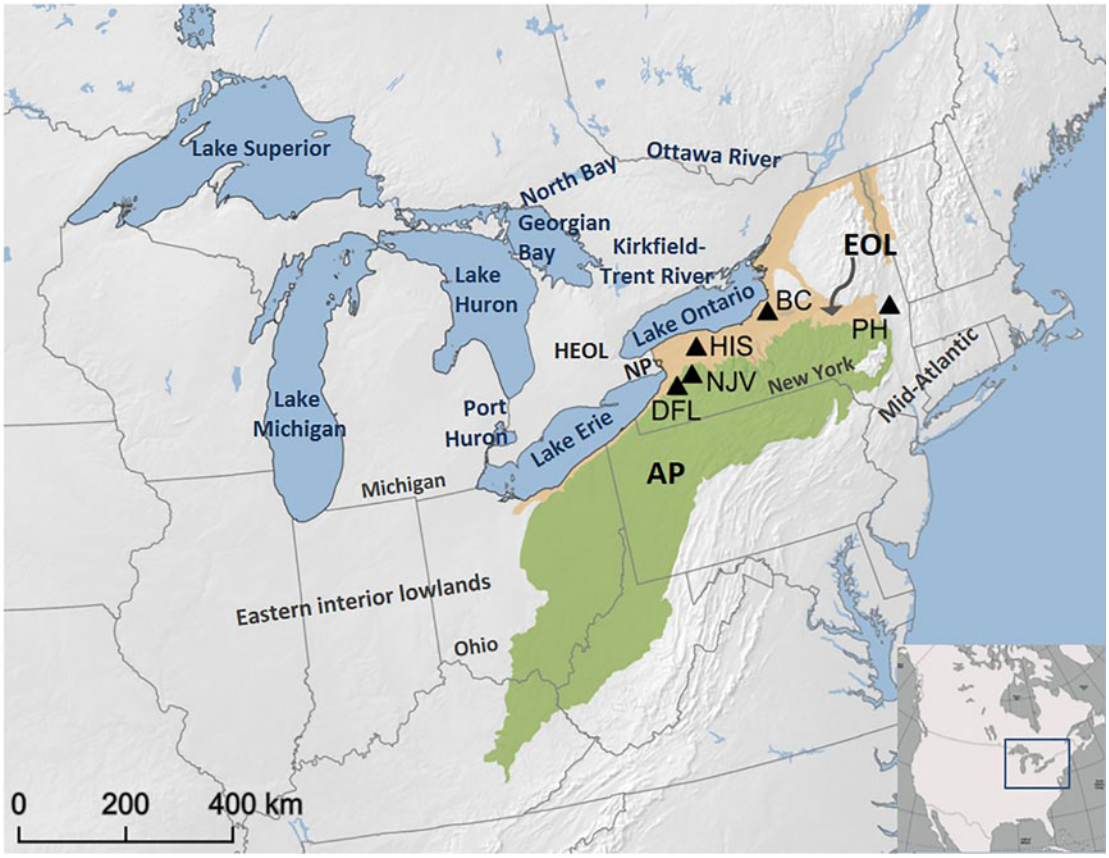

Figure 2. Map of the Great Lakes and study region, showing the lakes' configuration and modern drainage system. The five study sites (DFL, Doerfel; NJV, North Java; HIS, Hiscock; BC, Bell Creek; and PH, Pump House) are on the Erie and Ontario lowlands (EOL) and Allegheny Plateau (AP) in New York State, USA. HEOL, lowlands between Lakes Huron, Erie, and Ontario; NP, Niagara Peninsula.

west orientation, and the presence of Lakes Huron, Michigan, and Superior on their upwind sides (Sousounis and Fritsch, 1994; Scott and Huff, 1996; Weiss and Sousounis, 1999; Mann et al., 2002; Burnett et al., 2003; Villani et al., 2017; Lang et al., 2018).

During the LG interval, the changing oceans, ice sheets, glacial anticyclonic winds, and meltwater distribution affected synoptic-scale climate dynamics (e.g., Rind, 1987; Renssen et al., 2018; Conroy et al., 2019). The glacial Great Lakes certainly influenced mesoscale climate dynamics, but the physical characteristics and configuration of the lakes and ice sheet probably extended their influence on larger-scale dynamics to a regional scale (Long et al., 2007; Lowell et al., 2009; Rayburn et al., 2011; Ullman et al., 2014; Lewis and Anderson, 2017, 2019; Dalton et al., 2020; Figs. 3 and 4). The easterlies produced by glacial anticyclonic circulation extended ~150 km south of the LIS (Schaetzl et al., 2016 and references therein), forcing the prevailing westerlies to the south. This wind pattern included easterly winds across one or more of the glacial lakes at any given time and highly variable surface winds at the interface between easterlies and westerlies at ~100–200 km south of the ice sheet (e.g., Ullman et al., 2014; Schaetzl et al., 2016; Renssen et al., 2018; Renssen, 2020; Figs. 3 and 4). Prevailing westerlies were likely increasingly strong up to ~200 km from the easterly–westerly wind interface as their proximity decreased, then progressively moderate farther south. The extent of influence from the easterlies was perhaps ~300 km from the interface and 400–500 km from the LIS (e.g., Schaetzl et al., 2016; Figs. 3 and 4).

On the synoptic scale, atmospheric circulation and the prevailing westerlies upwind of the lakes were likely altered by the relative position of the LIS and Cordilleran Ice Sheet (CIS) and their associated winds (e.g., Rind, 1987; Atkinson et al., 2016; Utting et al., 2016; Figs. 3 and 4). From ~14.2 to 13.0 ka, the westerlies were the remains of the cool Pacific westerlies traveling across the Rocky Mountains; after 12.9 ka, the north-south corridor between ice sheets widened, and dry polar northwesterlies traveled around the glacial easterlies with limited orographic impact. The influence of warm southwesterly surface winds was likely minimal due to the strength of the prevailing westerlies south of the Great Lakes until after ca 11.5 ka in the Early Holocene interval (e.g., Edwards and Wolfe, 1996; Hostetler et al., 2000; Figs. 3 and 4).

The glacial Great Lakes may have amplified the already-increased seasonality of the LG interval (e.g., Berger, 1978; Solanki et al., 2004; Hegerl et al., 2011) due to their surface area, function as heat sink or heat source, and the significant differences in surface friction and albedo between frozen and open lake surfaces (Scott and Huff, 1996; Blanken et al., 2003; Rouse et al., 2003; Cordeira and Laird, 2008; Wright et al., 2012).

Paleoenvironmental reconstruction

Tamarack is rarely used in climate interpretations due to its limited representation in pollen records (e.g., Davis, 1969; Webb et al., 1978; Spear et al., 1994; Pisaric et al., 2001; Birks, 2003), which has made spruce species the primary indicators of boreal

https://doi.org/10.1017/qua.2021.76 Published online by Cambridge University Press

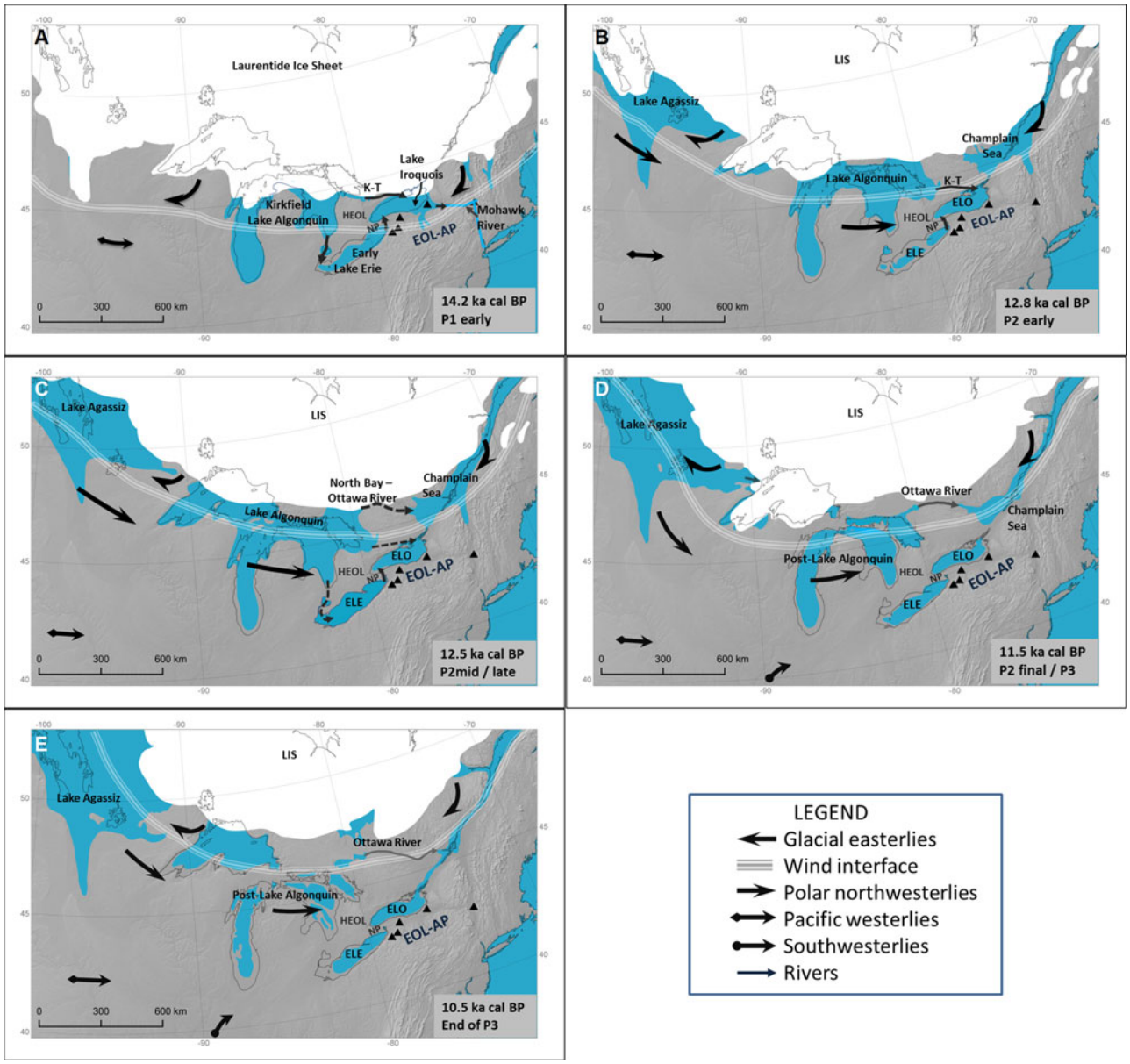

Figure 3. The paleogeography of the Great Lakes region in North America, 14.2–10.5 cal ka BP, illustrating changes in the lakes, position of the Laurentide Ice Sheet (LIS), meltwater distribution, and near-surface wind direction and speed over time. The approximate position of the easterly–westerly wind interface is at ~150 km from the LIS and ~50 km in width. (A) ~14.2 ka, the onset of phase P1: Lake Iroquois was expanding from meltwater directly off the LIS plus inflow from Early Lake Algonquin via Early Lake Erie (ELE), then via Kirkfield–Trent River (K-T) after ~13.8 ka. Winds across the Erie–Ontario lowlands–Allegheny Plateau (EOL-AP) were the glacial easterlies across Lake Iroquois and prevailing westerlies accompanying the Pacific air mass across ELE. (B) ~12.8 ka in P2early: Lake Iroquois and successor lakes were replaced by the initial Early Lake Ontario (ELO) and inflow continued from Lake Algonquin via K-T and ELE. Polar northwesterlies from around the western LIS were initiated. (C) ~12.5 ka at the P2early/P2mid transition, just before the North Bay–Ottawa River meltwater outlet opened from Lake Algonquin. Meltwater inflow into ELO was from Lake Algonquin via Kirkfield and perhaps ELE just before the opening of the new Lake Algonquin outlet. Northwesterlies were predominant across the EOL-AP. (D) 11.5 ka, P2 final/P3 transition. ELE and ELO attained their respective lowstands with the EOL-AP just within the southern reach of the unidirectional northwesterlies. (E) 10.5 ka, end of P3. The basins in the Great Lakes were all at their respective lowstands, and the wind interface was more than 300 km from the northern EOL-AP. (Maps accessed from Dyke et al. [2003], Dyke [2004], and Dalton et al. [2020], and revised by Keith Jenkins of the Cornell University Library GIS Services).

environments (e.g., Davis, 1969; Anderson, 1985; Jacobson et al., 1987; Dyke, 2005). Differences in the preferred habitats and tolerance of particular climatic and environmental conditions between tamarack and spruce suggest significant variations in moisture and temperature, particularly temperature extremes, on seasonal to multi-decadal timescales (e.g., Burns and Honkala, 1990; Vaganov et al., 1999; Jarvis and Linder, 2000).

Tamarack is a pioneer species, intolerant of shade and sustained drought; grows best in well-drained soils; and is more tolerant of frequent climate extremes than spruce (Harlow et al., 1979; Burns and Honkala, 1990 and references therein). White and black spruce (*Picea glauca* and *P. mariana*, respectively) are shade tolerant, but white spruce grows best on better-drained mineral soils, and black spruce grows in moister organic soils

https://doi.org/10.1017/qua.2021.76 Published online by Cambridge University Press

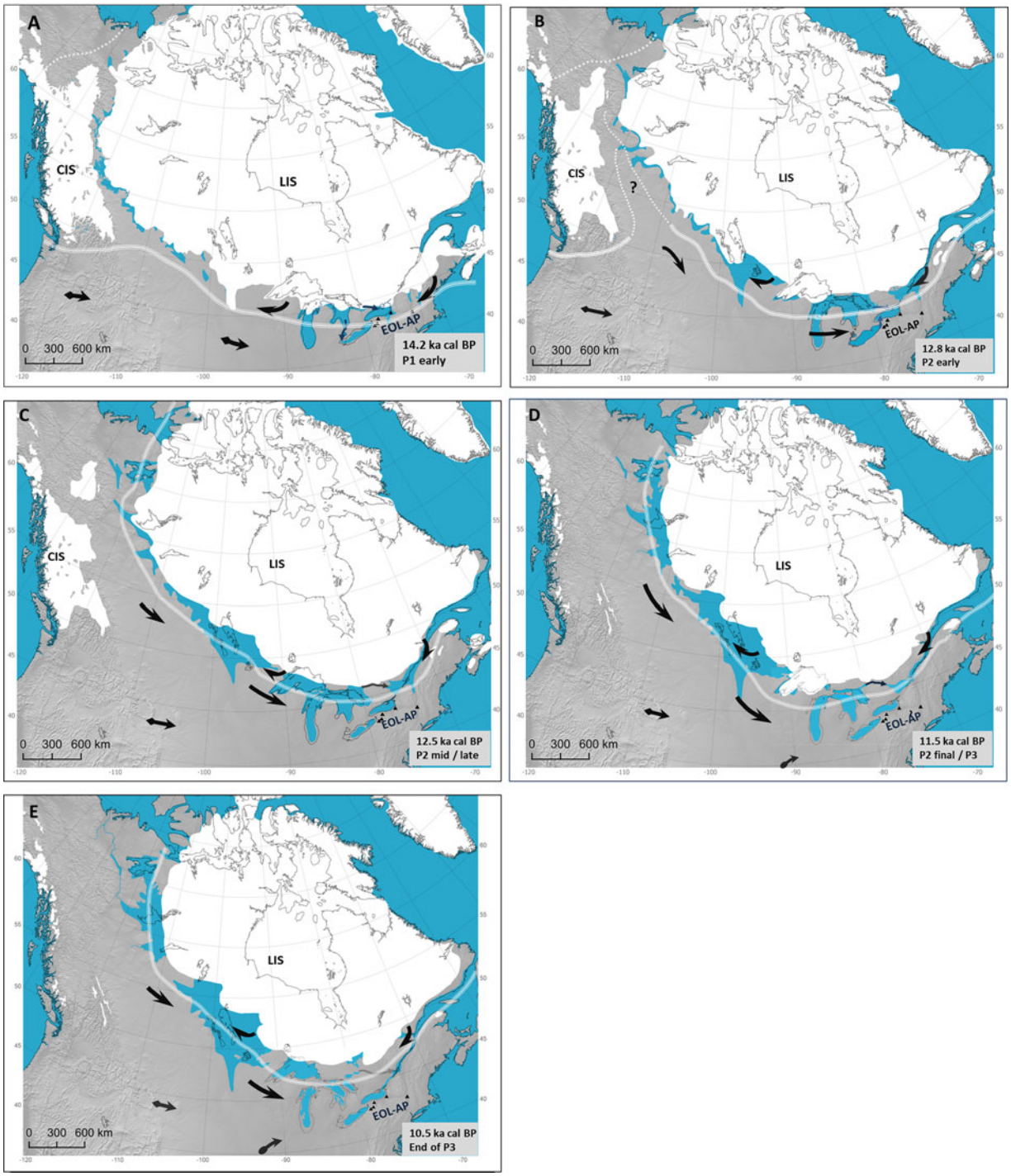

Figure 4. Proposed changes in wind sources and intensity across North America and their influence on the incoming winds across the Great Lakes during the late-glacial interval. The changes were derived from the position and movements of the Laurentide and Cordilleran Ice Sheets (LIS and CIS) and based on modern-day atmospheric circulation and glacial anticyclonic circulation (e.g., Rind, 1987; Schaetzl et al., 2016, Renssen et al., 2018; Conroy et al., 2019). (A) 14.2 ka, P1 interval. Glacial easterlies traveled across the northern half of the Erie–Ontario lowlands–Allegheny Plateau (EOL-AP). Incoming westerlies came directly from the Pacific Ocean and were relatively weak. (B) 12.8 ka, P2early. Easterlies were above the Lake Ontario basin and stayed approximately in that position until ca. 11.7 ka, and the Champlain Sea added to its moisture level. Dry polar northwesterlies began to influence the Great Lakes surface winds. (C) 12.5 ka, P2early to P2mid transition. Dry polar northwesterlies traveled around the near-perfect arc of the LIS and wind interface and across southern Lake Agassiz and the Great Lakes. Easterlies continued to receive moisture from the Champlain Sea. (D) 11.5 ka, P2final/P3 transition. The LIS had started to move northward from the lakes, but the Marquette readvance moved the wind interface southward. The EOL-AP was just within the southern reach of the unidirectional northwesterlies. The southwesterlies began to be a key factor in the climate of the Great Lakes region. (E) 10.5 ka, P3. The northwesterlies continued to influence the Great Lakes, but the wind interface was more than 300 km from the northern EOL-AP, which ended the GLEC in the study region. The legend is the same as in Fig. 3. (Maps from Dyke et al. [2003], Dyke [2004], and Dalton et al. [2020], revised by Keith Jenkins of the Cornell University Library GIS Services).

https://doi.org/10.1017/qua.2021.76 Published online by Cambridge University Press

Table 1. List of phases and subphases, samples, diameter, average ring widths of juvenile, mature, and complete sequences, species, chronology name if applicable, and radiocarbon ages.[a]

Phase	Site and sample	Diam (cm)	Juv ARW (mm)	Mat ARW (mm)	All ARW (mm)	N	Sp	Chronology	^{14}C Lab and number	^{14}C	^{14}C 1σ	Rings dated
P1 early	NJV 39	12.1	0.66	0.48	0.53	116	PCSP	NJV-I	Hd-22780	12,254	60	79–116
P1 early	NJV G24, 30, and F28	16.4	1.20	0.72	0.78	105	LALA	NJV-I	Hd-22596	12,064	44	52–61
P1 early	NJV 23 and G33	14.4	1.03	0.86	0.94	77	LALA	NJV-I				
P1 early	NJV F13	14.7	0.99	0.69	0.80	92	PCSP	NJV-I				
P1 early	NJV 19	19.6	0.94	0.78	0.73	134	LALA	NJV-I	Hd-22585	12,092	32	41–50
									Hd-25622	11,969	30	96–110
P1 early	NJV 38	10.0	0.68	0.38	0.42	120	PCSP	NJV-I				
P1 early	NJV F12	12.1	0.78	0.84	0.71	85	PCSP	NJV-I				
P1 early	NJV G21 and G34	12.1	0.91	0.44	0.47	129	PCSP	NJV-I	Beta-168586	11,970	80	11–40
									Hd-22597	11,902	51	21–30
									Hd-23635	12,046	74	71–115
P1 early	NJV 27	9.0	0.75	0.35	0.43	104	PCSP	NJV-I				
P1 early	NJV F32	16.0	1.41		1.11	72	LALA	NJV-I				
P1 early	NJV F17 and F33	11.2	0.72	0.47	0.45	124	PCSP	NJV-I	Hd-22782	12,030	45	2–30
									WW-8907	12,000	30	72–91
P1 early	NJV 26	11.8	1.15		0.82	72	LALA	NJV-I				
P1 early	NJV F43	11.7	1.09	0.45	0.72	81	LALA	NJV-I				
P1 late	DFL 9	10.0	0.70	0.36	0.50	126	LALA	DFL	CAMS-39330[b]	11,790	60	*Picea glauca* cone
P1 late	DFL 10	11.0	1.01	0.65	0.72	99	LALA	DFL	CAMS-43074[b]	11,550	60	*Picea glauca* cone
P1 late	DFL 12	10.4	0.62	0.69	0.57	135	LALA	DFL	Beta-122837[b]	11,390	100	*Fraxinus* wood
P1 late	DFL 11	9.2	0.70	0.40	0.51	94	LALA	DFL	CAMS-54734[b]	11,460	60	Mastodon bone
P1 late	NJV 32	12.0	0.78	0.47	0.54	111	PCSP	NJV-II				
P1 late	NJV F15	15.2	0.86	0.53	0.53	143	PCSP	NJV-II	Hd-22598	11,328	61	51–60
									Hd-22586	11,296	44	71–80
P2 early	HIS 1	12.2	1.52		1.35	41	PCSP		J5SW-38	11,020	50	NA
P2 early	BC 43	13.8	1.14	0.65	0.86	80	LALA	BC43 and 44				
P2 early	BC 44	18.6	1.32	1.14	1.19	78	PCSP	BC43 and 44	UCIAMS-178816	10,890	20	55–59
P2 early	BC 150	25.3	1.64	1.11	1.28	99	PCSP		UCIAMS-178820	10,545	20	1–5
									UCIAMS-161895	10,620	25	51–55

P2 mid	PH 12 and 16[c]	18.3	1.54		1.37	67	LALA		ISGS-A0529	10,350	40	NA
P2 mid	BC 50	23.0	1.16	1.38	1.26	91	LALA	BC mid	UCIAMS-163492	10,390	25	76–80
P2 mid	BC 238 and 239	28.9	1.78	1.32	1.32	110	LALA	BC mid	UCIAMS-178818	10,365	20	6–10
									UCIAMS-162637	10,380	25	88–97
P2 mid	BC 165	21.3	1.74	1.00	1.32	81	LALA	BC mid	UCIAMS-178817	10,365	20	35–39
P2 mid	BC 155	16.8	1.74		1.75	48	LALA		UCIAMS-163484	10,330	20	41–45
P2 mid	BC 208	12.4	1.54		1.11	56	LALA		UCIAMS-162633	10,355	25	49–53
P2 mid	BC 67	17.2	1.15		1.28	67	LALA		Hd-30251	10,308	32	15–25
P2 late	PH 17, 18, and 19	8.6	1.58		1.49	30	PCSP		ISGS-A0531	10,205	40	NA
P2 late	BC 63	16.1	0.99	0.99	0.99	81	LALA		Hd-30253	10,152	34	25–40
P2 late	PH 13 and 21[c]	8.8	1.26		1.26	35	LALA		ISGS-A0495	10,175	40	NA
									ISGS-A0496	10,175	45	NA
P2 late	BC 120	18.3	1.49	0.68	0.89	103	PCSP		UCIAMS-161893	10,140	25	84–100
									UCIAMS-178819	10,120	20	12–15
P2 late	BC 122 and 126	20.6	1.66	0.91	1.14	90	PCSP		UCIAMS-162648	10,155	25	79–94(β)
									UCIAMS-162632	10,185	25	79–94(α)
P2 late	PH 20	10.8	1.27		1.17	46	PCSP		ISGS-A0532	10,075	50	120–126
P2 late	BC 48	26.0	1.80	1.06	1.08	152	PCSP		Hd-30269	10,098	36	70–85
P2 late	BC 66	21.2	1.32	0.67	0.84	127	LALA		Hd-30271	10,204	34	16–25
									UCIAMS-163493	10,080	25	68–77
P2 final	BC 160	11.1	0.88	0.61	0.73	76	PCSP	BC trans				
P2 final	BC 215	20.4	1.62		1.48	69	PCSP	BC trans	UCIAMS-162635	10,035	25	62–66
P2 final	BC 216	26.8	1.28	1.37	1.29	104	LALA	BC trans				
P2 final	BC 35	16.1	1.38	0.73	1.02	79	PCSP	BC trans				
P2 final	BC 47	22.0	1.34	0.86	0.99	96	PSCP	BC trans				
P2 final	BC 65	20.0	0.94	0.96	0.79	119	PSCP	BC trans	Hd-28653	10,082	38	0–5
									Hd-30268	10,046	33	97–119
P2 final	BC 69	26.0	0.19	0.54	0.84	120	PCSP	BC trans	Hd-28656	10,125	38	36–45
P2 final	BC 76	10.4	1.08		0.80	65	PCSP	BC trans				
P2 final	BC 80	19.0	1.19	0.76	0.91	105	PCSP	BC trans				
P2 final	BC 81	22.8	1.66	0.96	1.14	100	LALA	BC trans				
P2 final	BC 161	19.9	0.59	0.97	0.72	139	PCSP	BC trans				

(*Continued*)

Table 1. (*Continued.*)

Phase	Site and sample	Diam (cm)	Juv ARW (mm)	Mat ARW (mm)	All ARW (mm)	N	Sp	Chronology	^{14}C Lab and number	^{14}C	^{14}C 1σ	Rings dated
P2 final	BC 159	13.2	0.88	0.72	0.79	84	PCSP	BC trans				
P3	BC 64	34.3	1.50	1.49	1.41	122	LALA		Hd-30270	10,011	44	7–25
									Hd-28655	9918	37	113–122
P3	BC 135	19.4	2.18		2.06	47	LALA		UCIAMS-161894	9980	25	41–45
P3	BC 68	25.1	1.93		1.84	68	LALA		WW8906	9995	30	67–68
P3	BC 224	10.6	0.60		0.8	66	LALA		UCIAMS-163491	9460	20	56–60
P3	BC 32	15.0	1.51		1.56	48	PCSP		Hd-30279	9403	35	24–48

[a]Abbreviations: Sites: NJV, North Java; DFL, Doerfel; HIS, Hiscock; BC, Bell Creek; PH, Pump House; Diam, diameter of the cross section; ARW, average ring width; Juv, Juvenile rings 1–35; Mat, mature rings 36–85; N, total ring count; Sp, species: PCSP, spruce species; LALA, tamarack; Rings dated, rings included in a 14C-dated segment, if known. Radiocarbon labs: Hd, Heidelberg; CAMS, Center for Accelerator Mass Spectrometry; WW, USGS Geoscience Center; UCIAMS, Keck Carbon Cycle AMS Laboratory; ISGS, Illinois State Geological Survey; Beta, Beta Analytic.
[b]DFL dates of findings found in situ above and below logs in analysis.
[c]PH logs are all tamarack, incorrectly listed as spruce in Miller and Griggs (2012).
N.B. NJV, BC, and PH are revised site abbreviations for WWW (Griggs and Kromer, 2008), OBF (Griggs and Grote, 2016, Griggs at al., 2017), and HM/HMPHS (Miller and Griggs, 2012), respectively. Sample numbers are the same.

(Sutton, 1969; Burns and Honkala, 1990). Unfortunately, the identification of white versus black spruce is difficult when using wood or pollen, which is problematic for interpretation of atmospheric moisture content, but the two species are easily identifiable in smaller macrofossils, especially cones or twigs (Harlow, 1959; Schweingruber, 1990; Hoadley, 1990). Tamarack tolerates extreme January temperatures of −55°C to −62°C, white and black spruce to −55°C, and the northern range limit of all three is where the average minimum January temperature (AMJT) is ∼ −30°C (Burns and Honkala, 1990; Supplementary Table S1). Of cool-temperate species, black ash and northern white-cedar (*F. nigra* and *Thuja occidentalis*, respectively) tolerate the coldest AMJT, ca. −18°C, but only black ash tolerates the same temperature extremes as spruce and tamarack, ca. −50°C (Kreyling et al., 2015; Strimbeck et al., 2015). The establishment and survival of any thermophilous species in a boreal climate generally depends on factors such as the length of the growing season and extremes in temperature, particularly at the beginning or end of the growing season (Burns and Honkala, 1990; Sperry et al., 1994; Vaganov et al., 1999; Jarvis and Linder, 2000; Mielko and Woo, 2006), and conifers plus diffuse-porous species such as black ash survive better than other arboreal species when frequent freeze–thaw events occur (Sperry et al., 1994).

The abundance of both pioneer tamarack and shade-tolerant spruce in the recovered logs and changes in their respective dominance over time plus the exclusivity of black ash offer a unique opportunity to identify changes in both environmental and climate conditions heretofore unknown.

MATERIALS AND METHODS

Materials

Subfossil logs were found at five LG sites in upstate New York (Fig. 2, Table 1). The Doerfel site (DFL) in Erie County (42.56° N, 78.71°W, 530 m above sea level [m asl]) and North Java (NJV) in Wyoming County (42.68°N, 78.33°W, 485 m asl) are spring-fed kettle ponds on the AP, and logs dating ca. 14.2–13.2 ka were recovered from the two sites (Laub and McAndrews, 1999, 2000; Griggs and Kromer, 2008; Laub, R.S., personal communication, 2006–2018; Fig. 2). The Hiscock site (HIS) in Genesee County (43.08°N, 78.08°W, 198 m asl) is composed of a spring-fed basin in the EOL with recovered wood fragments dating ca. 13.2 ka into the Early Holocene, but intact logs were rare due to the continual presence of wood-browsing mastodons (Laub et al., 1988; Laub, 2003a b; Laub, R.S., personal communication, 2006–2018). Bell Creek (BC) in Oswego County (43.30°N, 76.34°W, 135 m asl) and Pump House (PH) in Albany County (42.78°N, 73.70°W, 48 m asl) are floodplain sites on the Ontario and Mohawk Valley lowlands, respectively, and their recovered logs date from ∼12.8 ka into the Early Holocene (Miller and Griggs 2012; Griggs and Grote, 2016; Griggs et al., 2017; Fig. 2).

The logs recovered (used here) include 30 (15) at North Java, 6 (4) at Doerfel, 1 (1) at Hiscock, 58 (31) at Bell Creek, and 9 (4) at Pump House (Laub et al., 1988; Laub and McAndrews, 1999, 2000; Laub, 2003b; Griggs and Kromer, 2008; Miller and Griggs, 2012; Griggs and Grote, 2016; Griggs et al., 2017). Substantive pollen and other macrofossils were previously analyzed for Pump House, Hiscock, and Doerfel (Laub et al., 1988; Miller, 1988; Laub and McAndrews, 1999, 2000; Futyma and Miller, 2001; Laub, 2003b; Miller and Futyma, 2003; Miller and Griggs, 2012). An exploratory collection was analyzed for Bell

https://doi.org/10.1017/qua.2021.76 Published online by Cambridge University Press

Creek (Griggs and Grote, 2016; Griggs et al., 2017; Peteet, D.M., personal communication, 2015–2020), and North Java had no pollen analysis, but the site is within 20 km of Nichols Brook (Calkin and McAndrews, 1980; Karrow and Warner, 1988; Laub et al., 1988).

Methods

The 55 logs used in this study met three necessary criteria: presence of pith, at least 35 rings, and a pith-to-bark radius of >4 cm to omit possible branch growth. Species were identified and ring widths measured; several tree-ring chronologies were compiled (e.g., Cook and Kairiukstis, 1990; Hoadley, 1990; Schweingruber, 1990; Griggs and Kromer, 2008; Miller and Griggs, 2012; Table 1), but only one chronology, 211 years in length, had the sample depth of 10 or more per year that is necessary for annual climate reconstruction (Griggs et al., 2017). This made annual climate reconstruction not viable for this study. Rather, based on our initial observations and using the biological ages of rings from pith to bark, the average ring widths (ARWs) of juvenile growth in rings 1–35 from the pith and mature growth in rings 36–85 were calculated and compared for possible evidence of environmental and climate changes on a multi-decadal timescale (e.g., Vaganov et al., 1999; Jarvis and Linder, 2000). Box-and-whisker diagrams were used to identify changes, and two-tailed *t*-tests were used to identify significant changes in the ARWs over time.

For an assessment of climate conditions in the study interval, juvenile and mature ARWs were calculated from ring widths of 453 white spruce trees in 22 stands that cover most of the north-south range of white spruce across central and eastern Canada (International Tree-Ring Data Bank [ITRDB], available at https://www.ncdc.noaa.gov/data-access/paleoclimatology/tree-ring, accessed 2015–2019). Similar data were not available for tamarack or black spruce (Supplementary Fig. S1, Supplementary Table S1). The southern boundary of white spruce runs at approximately the 20° C average summer isotherm (Burns and Honkala, 1990), and the ARWs of white spruce were divided into 12 groups by the approximate distance of their respective sites to the southern boundary of the species range at the same longitude to acquire a data set representing relatively warmer summer temperatures on a N-S transect ending at the southern boundary. Those ARWs were used as representatives of spruce growing in northern, central, and southern boreal-type climates.

A timeline of possible climate changes in the LG interval was established from ^{14}C dates of logs in situ at key stratigraphic positions and/or those with tree-ring growth patterns matching patterns in other dated samples and from ^{14}C dates of additional materials associated with the logs. The ^{14}C dates were calibrated and the 2σ calibrated error range was determined using the IntCal20 radiocarbon calibration curve (Reimer et al., 2020) and OxCal v. 4.3 software (Bronk Ramsey et al., 2001; http://c14.arch.ox.ac.uk/oxcal.html accessed 2020–2021) (Fig. 5). Several clusters of dates suggested by the calibrated years were used to group the samples into temporal phases, either where gaps between clusters were more than 100 years long or between a chronology and samples with no matching growth patterns.

To test for climate change over time, the mean values of the ARWs in the main phases were tested for significant differences between phases using the box-and-whisker diagrams and two-tailed *t*-tests. The data sets of each phase were further divided by species and by sites to test for the possible influence of those factors on any significant differences between phases. The mean values and range of juvenile and mature ARWs of the main phases were also compared with the modern boreal forest data using the box-and-whisker diagrams to find whether they represented a northern, central, or southern boreal-type climate.

The main phases were then split into subphases in which smaller clusters were separated by less than 100 years, represented a tree-ring chronology, or contained only a few samples over a multi-century period. The mean values of the subphase ARWs were similarly tested for climate changes between subphases within and between the main phases.

Species representation of all logs plus other proxy records, including pollen, macrofossil, Coleoptera, firn, till, and eolian deposits found at sites within and immediately west, southwest, and northeast of the EOL-AP are included in this study (e.g., Morgan, 1972; Anderson, 1985; Filion, 1987; Fritz et al., 1987; Shane, 1987; David, 1988; Shane and Anderson, 1993; Tinkler and Pengelly, 1994; Laub, 2003b; Anderson and Lewis, 2012; Schaetzl et al., 2013; Watson et al., 2018; Fastovich et al., 2020; Young et al., 2020). They are used in interpreting climate change and the extent of the lake-effect climate using features such as the modern range of their respective species, their capability of withstanding climate extremes, and/or their physical characteristics.

RESULTS

Of the 55 samples meeting the necessary criteria, 27 are tamarack and 28 spruce (Table 1). For all samples, the ARWs range from 0.62 to 2.18 mm for the juvenile data and from 0.35 to 1.49 mm for the mature data (Table 1) with a slightly higher range of tamarack ARWs (for the juvenile segments: tamarack, 0.62–2.18 mm; spruce, 0.66–1.80 mm; for the mature rings: tamarack, 0.36–1.49 mm; spruce, 0.35–1.14 mm; Table 1). The modern ARWs of white spruce range from 0.05 to 4.10 mm (juvenile) and 0.05 to 3.50 mm (mature), suggesting that these trees grew in climate conditions typical of the boreal region today.

Forty-seven ^{14}C dates were taken from one or more segments of rings in 33 of the 55 samples, and the other 22 samples were placed in time by their association with other dated samples and other materials (Fig. 5, Table 1). From their distribution and clustering on the calibration curve, three main phases, P1 at 14.2–13.1 ka, P2 at 12.9–11.5 ka, and P3 at 11.5–10.5 ka, were chosen (Fig. 5, Tables 1 and 2), all of which are over the 200+ year length considered necessary to represent regional rather than local climate change (e.g., Bartlein et al., 1986).

A significant increase in both juvenile and mature ARWs from P1 to P2 is indicated by the box-and-whisker diagrams and *t*-tests between phases and between species and sites within phases (Fig. 6A–C, Table 3A–F). A northern boreal-type forest is suggested by the ARWs of P1 and a southern boreal-type forest by the ARWs of P2 (Fig. 6). The ARWs show a slight increase from P2 to P3 (Fig. 6A–C), suggesting climate conditions farther south than in P2 (Fig. 7), but the *t*-test is insignificant, and the small sample count and representation of only one site in P3 leaves any interpretation of change between P2 and P3 tentative only.

Phases P1 and P2 were divided into six subphases by smaller clusters and chronologies: P1early and P1late and P2early, P2mid, P2late, and P2final (Figs. 5 and 6D, Table 2). All subphases are also at or over the 200 year minimum length requirement for representing regional change.

https://doi.org/10.1017/qua.2021.76 Published online by Cambridge University Press

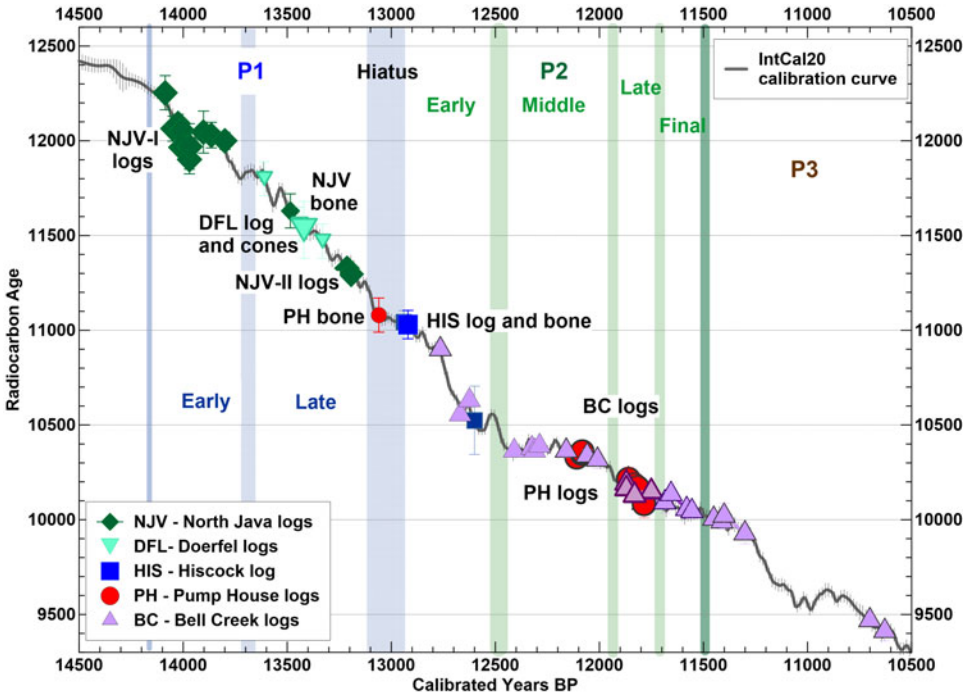

Figure 5. The placement of the 47 radiocarbon dates from 33 samples, additional macrofossils, and associated bones (Table 1) on the IntCal20 calibration curve (Reimer et al., 2020). Shaded columns are at the start of P1 and between phases and subphases. The wide column represents the hiatus of wood samples between P1 and P2; the date within the hiatus is of bone from the Hiscock site. The radiocarbon error bars are at the 2σ level and not visible where the range is smaller than the symbol. Bones and cone dates are represented by the smaller symbols of the corresponding site.

There is no significant change in ARWs between subphases P1early and P1late, although a slight decrease in the ARWs is suggested in the box-and-whisker diagrams (Fig. 6D, Table 3D1). As expected from the positive trend between main phases P1 and P2, the progression from a northern to southern boreal forest is evident between subphases P1late and P2early (Fig. 6D, Table 3D2). Within P2, the only significant differences in ARWs are a possible increase from P2early to P2mid and a significant decrease from P2mid to P2late and P2final (Fig. 6D, Tables 2 and 3D1). Only tamarack is represented in P2mid (Table 2), but *t*-tests between the ARWs of P2mid and in the other P2 subphases showed that the increase and decrease are not species specific (Fig. 6D, Table 3E). The increase and significant *t* -tests between ARWs of subphase P2final and P3 (Fig. 6D, Table 3D2) supports the transition from a southern to more southern boreal climate suggested between the ARWs of P2 and P3.

For species representation, more than 90% of all recovered logs and macrofossils from the five study sites are tamarack or spruce, and the two species are equally represented, except at Pump House, where tamarack, spruce, and balsam fir (*Abies balsamea*) are equally represented (Miller and Griggs, 2012; Table 1). During all phases and subphases, tamarack and spruce are suggested to be codominant, except for the exclusivity of tamarack logs in P2mid and the dominance of spruce in P2final (Table 2). Other tamarack macrofossils were present at all sites, and pollen representation was predictably low (Laub and McAndrews, 1999, 2000; Miller and Griggs, 2012; Peteet, D.M., personal communication, 2015–2020). Recovered spruce cones and other identified macrofossils represent only white spruce at Bell Creek and Pump House (*P. glauca*; Laub and McAndrews, 1999, 2000; Miller and Griggs, 2012; Griggs and Grote, 2016). Significant variations in spruce pollen percentages during ~P2mid into P3 were evident at Bell Creek (Peteet, D.M., personal communication, 2015–2020).

In the other ~10% of logs dating from 14.2 to at least 11.9 ka, species include the boreal species of balsam fir, poplar, and paper birch (*A. balsamea*, *Populus* spp., *Betula papyrifera*, respectively) plus black ash which dates back to at least ~13.25 ka (Laub and McAndrews, 1999). In the upper LG and lower EH deposits, ~11.9 to 10.5 ka, around 50% of the logs are spruce or tamarack, with an increase in balsam fir and black ash and the first representation of the thermophilous northern white-cedar, red and eastern white pine, American elm, and red maple (*T. occidentalis*, *Pinus resinosa*, *P. strobus*, *Ulmus americana*, and *Acer rubrum*, respectively; Laub et al., 1988; Griggs and Kromer, 2008; Miller and Griggs, 2012; Griggs and Grote, 2016; Griggs, C.B., unpublished data).

Four takeaway points from the results are evident. First is the three main phases and six subphases identified from high-resolution ^{14}C dating and significant differences in ARWs and species representation over time. Second is the major change in ARWs between P1 and P2 that suggests a transition from northern to southern-type boreal climate, both with possible non-analog features. Third is the minor changes in ARWs and species presence between several subphases. Fourth is the abundance of tamarack and sole representation of black ash for thermophilous species, in addition to spruce. All points support the interpretation of lake-effect climate in the following sections.

EVOLUTION OF ENVIRONMENT AND CLIMATE

In this section, the GLEC and its progression over time are interpreted from changes in the ARWs, species representation, and other proxy records from both the EOL-AP and the lowlands between the Lake Huron, Erie, and Ontario basins (HEOL; Fig. 2). The interpretations are extrapolated to the southwestern AP and interior lowlands (Fig. 2) to examine possible changes in the extent of the lakes' effects on climate over time.

Phase 1 (P1), ~14.2–13.1 ka

P1early, ~14.2–13.8 ka

The ARWs in P1early suggest the northern boreal climate of today (Fig. 7, Table 2), but the exclusivity of black ash for cool-

https://doi.org/10.1017/qua.2021.76 Published online by Cambridge University Press

Table 2. Summary of the data sets within phases and subphases: range of dates, average and sample counts of the juvenile and mature average ring widths (ARWs), and represented species for each time interval.

	Dates	ARW, mm		Sample count		Species count[a]	
Phase	cal ka BP	Juvenile	Mature	Juvenile	Mature	Tamarack	Spruce
P1	14.2–13.1	0.89	0.56	19	17	10	9
P2	12.9–11.5	1.35	0.92	31	21	13	18
P3	11.5–10.5	1.54	1.49	5	1	4	1
Subphases							
P1early	14.2–13.7	0.95	0.59	13	11	6	7
P1late	13.6–13.1	0.78	0.52	6	6	4	2
P2early	12.9–12.5	1.41	0.97	4	3	1	3
P2mid	12.5–11.9	1.52	1.23	7	3	7	0
P2late	11.9–11.7	1.42	0.86	8	5	3	5
P2final	11.7–11.5	1.17	0.85	12	10	2	10

[a]The species counts suggest co-dominance, except in P2mid, where only tamarack was represented, and P2final, when spruce was likely dominant.

temperate species suggests a more central boreal zone that is the northern boundary of that species' range today. A northern boreal climate is also seen in the high dominance of spruce with minimal thermophilous species in many pollen records from the EOL-AP and HEOL (e.g., Miller, 1973; Yu, 2000; Futyma and Miller, 2001; Miller and Futyma, 2003; Dyke, 2005), but both northern and southern boreal-type summer ecozones are suggested by Coleoptera species, agreeing with the warmer summer conditions suggested by the black ash (Edwards et al., 1985; Fritz et al., 1987). These proxies suggest a non-analog northern boreal environment and high seasonality between summers and winters, possibly greater than caused by the solar and orbital forcings alone.

P1late, ~13.7–13.1 ka

Moister and perhaps slightly cooler growing conditions in a north-central boreal climate are suggested by the minimum ARWs of P1late but are not significantly different from P1early (Fig. 6D, Table 3D1). However, moister and cooler conditions are supported by substantial ice accumulation in the western EOL-AP and permafrost, oxygen isotopes, and firn on the Niagara Peninsula (Miller, 1973; Mott and Farley-Gill, 1978; Edwards et al., 1985; Tinkler and Pengelly, 1994; Young et al., 2020).

The hiatus, ~13.1–12.9 ka

The increase in ARWs between P1 and P2 suggests a transition from northern boreal- to southern boreal-type climate (Fig. 7), but the lack of logs gives no higher temporal resolution to this change, thus the term "hiatus." A transition to warmer and drier summer conditions is suggested in Coleoptera and a few pollen records (Miller and Morgan, 1981; Edwards et al., 1985; Fritz et al., 1987; Motz and Morgan, 2001; Webb et al., 2003). Warmer and drier conditions are also plausible in the reduction of ice and firn in the EOL-AP and HEOL (e.g., Miller, 1973; Edwards et al., 1985; Fritz et al., 1987; Tinkler and Pengelly, 1994; Young et al., 2020).

Phase 2 (P2), ~12.9–11.5 ka

In P2, the ARWs plus Coleoptera species suggest a southern boreal-type ecozone for summer in the EOL-AP and HEOL (Edwards et al., 1985; Fritz et al., 1987; Miller and Morgan, 1981, Motz and Morgan, 2001; Fig. 7). However, the continuing exclusivity of black ash in most if not all of P2 suggests conditions such as colder and more variable winter temperatures and/or frequent freeze–thaw events during the growing season prohibited the establishment of additional thermophilous species.

The transition to a southern boreal summer climate between P1 and P2 sometime between 13.1 and 12.9 ka directly contrasts with the 12.9 ka transition from the warming BA to colder YD climate outside the lakes region (Fig. 1). The increase in annual variability in climate conditions and/or in seasonality from warming summers to continuing cold winters suggests that the annual cycle of open and frozen lakes plus length of transitions between the two were primary factors in GLEC dynamics.

P2early, ~12.9–12.5 ka

The ARWs indicate a southern boreal-type climate in summer, but species representation continues to suggest harsh winters in P2early. In Webb et al. (2003), a significant warming of both summer and winter temperatures in the western EOL-AP is based on changes in pollen percentages, but the non-inclusion of tamarack due solely to its low representation in pollen records likely exaggerated the proposed increase in summer temperatures and certainly raises questions about an increase in winter temperatures.

P2mid, ~12.5–11.9 ka

An increase in flooding or other environmental disturbance and/or more frequent climate extremes is suggested by the higher ARWs and exclusivity of tamarack (Fig. 6D, Tables 2 and 3E), both indicators of an open landscape and frequent site disruption for the ~600 year duration of P2mid. The higher ARWs suggest warmer temperatures, but the open terrain may be the main factor for good growth. The disturbances and extremes are also suggested by a slight decrease in spruce pollen, an increase in tamarack needles, and/or higher percentages of non-arboreal pollen across the EOL-AP and HEOL (e.g., Miller, 1973; Fritz et al., 1987; Karrow and Warner 1988; Tinkler et al., 1992; Yu, 2000). Similarly, an open environment with flowing water in a southern boreal/cool-temperate summer climate is suggested by Coleoptera species (Fritz et al., 1987; Calkin and McAndrews, 1980, Miller and

https://doi.org/10.1017/qua.2021.76 Published online by Cambridge University Press

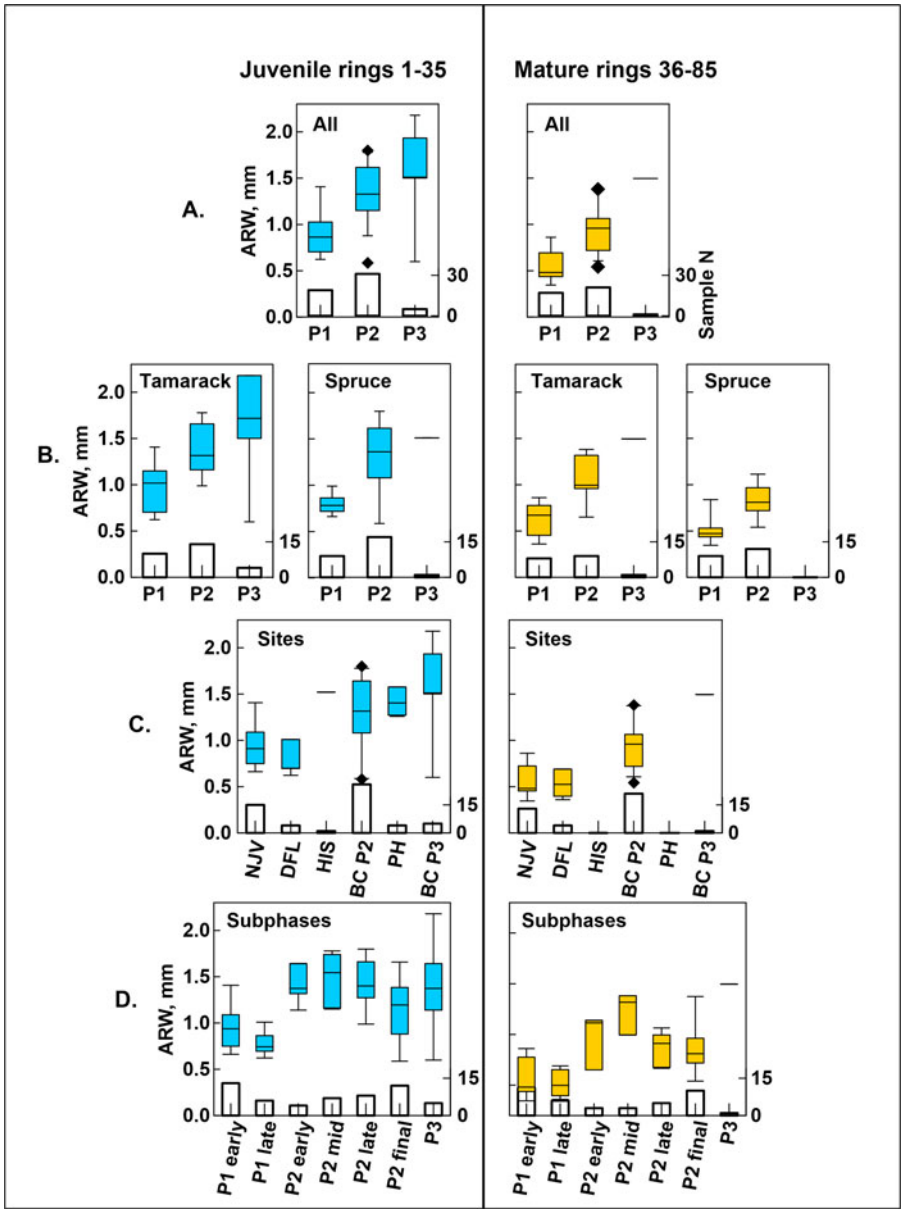

Figure 6. Box-and-whisker diagrams of the juvenile and mature average ring width (ARW) data sets. (A) ARWs in the three main phases. (B) ARWs further divided by species; (C) ARWs divided by phases and sites: North Java (NJV) and Doerfel (DFL) are in P1; Hiscock (HIS), Bell Creek (BC), and Pump House (PH) are in P2; and the Early Holocene (EH) samples from BC are in P3. (D) ARWs of samples in the six subphases and EH. The supporting *t*-statistics and *P* values are listed in Table 3. The boxes contain the 2nd and 3rd quartile data points; the horizontal lines are the median values; whiskers include at least 90% of the data points; diamonds represent outliers. Single horizontal lines (no box) represent the ARW of one sample. The bar charts along the x-axis of each diagram represent the sample counts per data set with its scale on the right y-axis.

Morgan, 1981; Motz and Morgan, 2001). Harsh winters continued to restrict establishment of additional cool-temperate species.

P2late, ~11.9–11.7 ka

A return to a less variable, drier climate and the succession of pioneer to climax tree species in P2late is indicated by the ARWs, equivalent to the ARWs of P2early, and codominance of spruce and tamarack (Figs. 1 and 6, Table 2). Drier conditions are also indicated by the represented Coleoptera species (e.g., Fritz et al., 1987). Harsh winters continued.

P2final, ~11.7–11.5 ka

The dominance of spruce and reduced ARWs indicate a more closed forest in a climax environment, with tamarack growing mainly along streambanks or shorelines, suggesting the continuation of the drier and less variable southern boreal-type conditions. A less variable climate is also indicated by substantial forest floor litter and the continuation of the same Coleoptera species. No abrupt climate change is indicated by the ARWs or annual ring growth during the LG-EH transition, ca 11.7–11.5 ka (Griggs et al., 2017). However, an alleviation of the harsh winters may have begun by the end of this phase, suggested by the increase of thermophilous species from the upper LG/lower EH deposits.

Phase 3 (P3), ~11.5–10.5 ka

The tentative increase in ARWs only suggests a transition from a south-central boreal to a mixed boreal/cool-temperate ecosystem by the start of this phase (Figs. 1, 6A, and 7, Tables 2 and 3D2), but the transition and decreased seasonality is clearly indicated by the decrease in tamarack and spruce and the additional thermophilous species in the logs. These conditions suggest the end of the GLEC in the EOL-AP region.

PROPOSED ROLE OF LAKE-EFFECT PROCESSES ON CLIMATE

Here we give an interpretation of the glacial lakes' effects on climate, including the inception, changing dynamics, and demise of the GLEC based on the evolution of climate discussed earlier

https://doi.org/10.1017/qua.2021.76 Published online by Cambridge University Press

Table 3. The results of the *t*-tests used to identify significant differences in the mean values of the juvenile and mature average ring widths (ARWs) between the phases, species, sites, and subphase data sets over time (Fig. 6).[a]

			Juvenile			Mature		
Data sets	Phases / sites compared		*t*-test	Probability	Sample N's	*t*-test	Probability	Sample N's
A. Between phases (Fig. 6A)								
All samples	P1	P2	**4.485**	*P < 0.01*	19 |31	**5.055**	*P < 0.01*	17 | 21
	P1	P3	**4.025**	*P < 0.01*	19 | 5	Too few		17 | 1
	P2	P3	1.2057	NS	31 | 5	Too few		21 | 1
B. Between phases for each species (Fig. 6B)								
Tamarack	P1	P2	**3.918**	*P < 0.01*	10 | 14	**3.774**	*P < 0.01*	8 | 9
	P1	P3	**2.351**	*P < 0.05*	10 | 4	Too few		8 | 1
	P2	P3	0.71	NS	14 | 4	Too few		9 | 1
Spruce	P1	P2	**3.013**	*P < 0.01*	9 | 17	**4.093**	*P < 0.01*	9 | 12
	P1	P3	Too few		9 | 1	Too few		9 | 0
	P2	P3	Too few		17 | 1	Too few		12 | 0
C1. Between sites in each phase (Fig. 6C)								
P1	NJV	DFL	−1.47	NS	15 | 4	−0.486	NS	13 | 4
P2	BC	PH	0.716	NS	26 | 4	Too few		21 | 0
	BC	HIS	Too few		26 | 1	Too few		21 | 0
	PH	HIS	Too few		4 | 1	Too few		0 | 0
C2. Between sites in different phases (Fig. 6C)								
P1 x P2	NJV	BC	**2.908**	*P < 0.01*	15 | 26	**4.387**	*P < 0.01*	13 | 21
	NJV	PH	**4.115**	*P < 0.01*	15 | 4	Too few		13 | 0
	DFL	BC	**2.399**	*P < 0.05*	4 | 26	**3.037**	*P < 0.01*	4 | 21
	DFL	PH	**5.4301**	*P < 0.01*	4 | 4	Too few		4 |0
P1 x P3	NJV	EH	**3.4885**	*P < 0.01*	15 | 5	Too few		13 | 1
	DFL	EH	**2.5031**	*P < 0.05*	4 | 5	Too few		4 | 1
P2 x P3	BC	EH	1.324	NS	26 | 5	Too few		25 | 1
	PH	EH	0.437	NS	4 | 5	Too few		0 | 1
D1. Between subphases within P1 and P2 (Fig. 6D)								
P1	P1early	P1late	−1.648	NS	13 | 6	−0.808	NS	11 | 6
P2	P2early	P2mid	1.335	NS	4 | 7	*2.066*	*P < 0.10*	3 | 3
	P2early	P2late	0.904	NS	4 | 8	*0.264*	NS	3 | 5
	P2early	P2trans	−0.619	NS	4 | 12	*0.332*	NS	3 | 10
	P2mid	P2late	−0.742	NS	7 | 8	***−2.638***	*P < 0.05*	3 | 5
	P2mid	P2trans	**−2.44**	*P < 0.05*	7 | 12	***−2.507***	*P < 0.05*	3 | 10
	P2late	P2trans	−1.989	*P < 0.10*	8 | 12	−0.117	NS	5 | 10
D2. Consecutive subphases between P1 and P2, and P2 and P3								
P1 x P2	P1late	P2early	**5.531**	*P < 0.01*	6 | 4	***3.442***	*P < 0.05*	6 | 3
P2 x P3	P2final	P3	1.81	*P < 0.10*	12 | 10	Too few		5 | 1
E. Tamarack in P2mid vs other tamarack and vs all others in P2								
P2	P2mid	P2 tamarack	**−2.861**	*P < 0.05*	7 | 9	***−4.008***	*P < 0.05*	3 | 8
	P2mid	P2 all others	−1.87	*P < 0.10*	7 | 24	***−2.893***	*P < 0.01*	3 |18

[a]Positive *t*-values indicate an increase in ARWs from the left to right of compared data sets and vice versa. Bold values indicate significantly different data sets with $P < 0.01$ or 0.05; standard font indicates significant values at $P < 0.10$; "NS" indicates that the data sets are not significantly different. The tests contain ≥ 4 samples in both data sets except for the italicized *t*-values where one of the data sets has only 3 samples and the "Too few" tests where one or both data sets have < 3 samples.

https://doi.org/10.1017/qua.2021.76 Published online by Cambridge University Press

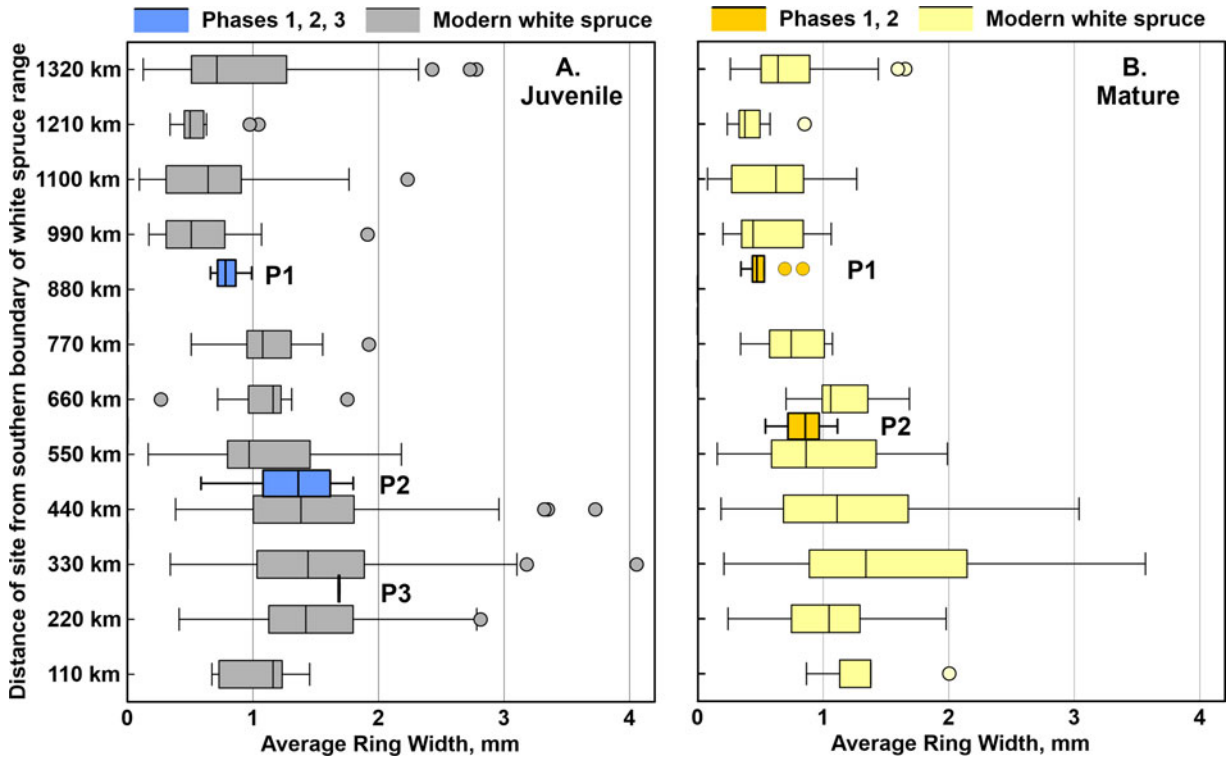

Figure 7. The spruce ARWs from this study compared with those of samples from more than 500 white spruce trees in boreal forests across central and eastern Canada, North America (International Tree-Ring Data Bank [ITRDB], https://www.ncdc.noaa.gov/data-access/paleoclimatology/tree-ring, accessed 2015–2019) in box-and-whisker plots (see Fig. 6 caption). The y-axis is the approximate distance from the southern boundary of the range of white spruce to the location of each modern site at the same longitude. Only spruce samples were tested here due to the limited tamarack data on the ITRDB (Supplementary Fig. S1, Supplementary Table S1).

and our current understanding of the glacial lake system and change plus ice sheets, meltwater, topography, and associated winds. Finally, we discuss the significance of the presence of both tamarack and black ash and its implications for the interpretation of the GLEC in the Great Lakes region and in climate reconstruction in general.

Onset of the GLEC

The GLEC across the EOL-AP likely began when easterlies traveled across the deglaciated Lake Erie basin onto the interior lowlands west of the EOL-AP before deglaciation of the Lake Ontario basin, but the single lake and wind direction was likely insufficient to produce a regional-scale regime (Laird et al., 2009). More likely, the lake-effect climate was initiated from the northward expansion of Lake Iroquois (Fig. 3A) and northward movement of the easterly–westerly wind interface resulting in easterlies across Lake Iroquois and westerlies across Early Lake Erie (ELE; Fig. 3A). Changes in the lake-effect climate system in the following years, ca 14.2–10.5ka, are based on probable linkage of changes in climate to those in the hydrologic and glacial conditions. The following interpretations are rough estimates of those linkages.

Phase 1, ~14.2–13.1 ka

P1early, ~14.2–13.8 ka

The northern boreal climate suggested by the ARWs and species representation coincided with an expanding Lake Iroquois, ELE, and meltwater drainage through the EOL-AP via the Mohawk and Hudson Rivers (Eschman and Karrow, 1985; Kaiser, 1994; Lewis et al., 2012; Lewis and Anderson, 2019; Fig. 3A). The wind interface was located across the EOL-AP, with Lake Iroquois to the north of the interface and ELE to the south (Dyke et al., 2003; Dalton et al., 2020; Fig. 3A). Easterlies traveled across the ~300 km fetch of Lake Iroquois and westerlies across the ~350 km fetch of ELE and likely produced copious amounts of precipitation along the interface, especially in the fall, when lakes were heat sources and evaporation rates were high and air temperatures were lower than water temperatures. The effects of open versus frozen lakes on the surface winds induced a greater seasonality.

P1late, ~13.7–13.1 ka

The cooler and/or wetter climate conditions suggested by the proxy records is coincidental with the expansion of Lake Iroquois to the north and east and continuing drainage into the Mohawk River Valley in the EOL-AP. The direct meltwater input from the LIS into Lake Iroquois was replaced by input via the much shorter Kirkfield-Trent Valley route to the north of the lake, which brought cooler meltwater into the lake than did meltwater input via ELE (Eschman and Karrow, 1985; Kaiser, 1994; Lewis et al., 2012; Lewis and Anderson, 2019; Fig. 3A). Meltwater inflow into ELE had ceased ca. 13.8 ka BP, which increased that lake's temperature and evaporation rate, but the end of meltwater inflow also reduced the size and output of the ELE, which in turn reduced its influence on the westerly winds, surface air temperatures, and perhaps the spatial extent of the GLEC (Eschman and Karrow, 1985; Coakley and Lewis, 1985; Tinkler et al., 1992; Lewis et al., 2012).

https://doi.org/10.1017/qua.2021.76 Published online by Cambridge University Press

To the east, the Champlain Sea was expanding, which increased the level of moisture in the easterlies (e.g., Pair and Rodrigues, 1993; Rayburn et al., 2011). At the wind interface, the extra moisture in both winds plus the higher temperature in the westerlies and lower temperature in the easterlies produced copious amounts of precipitation in the HEOL and EOL-AP. An ice advance in the western EOL-AP at 13.3–13.0 ka, the end of P1late into the hiatus, is proposed by Young et al. (2020). Those dates were estimated from findings at sites along the Genesee River and Cattaraugus Creek floodplains in the western AP, but the 2σ ranges of calibrated dates of wood and bone are ca. 13.8–13.2 ka at Doerfel located < 20 km Cattaraugus Creek, ca. 13.5–13.1 ka at North Java II between the two floodplains, and ca. 13.2–12.6 ka for the oldest dates at Hiscock at ~50 km west of the Genesee River floodplain. The ranges of these dates indicate an overall ice-free landscape on at least the higher elevations and relatively flat terrains from 13.3 to 13.0 ka. A possible alternative to an ice advance may have been increased precipitation and significant but isolated ice accumulations on the floodplains and more variable terrain. The suggested minimum ARWs plus ice accumulation and permafrost in both the EOL-AP and on the Niagara Peninsula (NP; Miller, 1973; Edwards et al., 1985; Tinkler and Pengelly, 1994; Young et al., 2020) in P1late suggest that the expansion of Lake Iroquois and reduction of ELE may have pushed the wind interface farther south onto the EOL-AP. The minimum ARWs and possible maximum ice accumulation on the EOL-AP (Young et al., 2020) date to around the end of P1late and are also coeval with a brief but intense outburst of meltwater from Lake Agassiz that flowed briefly into ELE sometime between 13.2 and 12.9 ka and may have contributed to a cold and moist climate during the end of P1late and into the hiatus (Morgan, 1972; Eschman and Karrow, 1985; Farrand and Drexler, 1985; Teller, 1987; Tinkler et al., 1992; Rayburn et al., 2011; Leydet et al., 2018).

The hiatus, ~13.1–12.9 ka

A change in GLEC from a northern to southern boreal-type and drier climate, suggested by the increase in ARWs from P1 to P2 and in changes in other proxy records, is coeval with the transition of Lake Iroquois to progressively smaller lakes from the rerouting of its output to the NE corner of the Lake Ontario basin, ending meltwater drainage via the Mohawk River into the EOL-AP (Pair and Rodrigues, 1993; Dyke et al., 2003, Rayburn et al., 2005, 2011; Anderson and Lewis, 2012; Lewis and Todd, 2019; Lewis and Anderson, 2019; Dalton et al., 2020; Fig. 3A and B). These changes alone likely increased summer temperatures and length of the growing season, but the wind interface was also moving north (Fig. 3A and B). By the end of the hiatus, both the Lake Ontario basin and ELE were south of the wind interface, which ended the copious amounts of precipitation across the EOL-AP and HEOL. However, the overall reduction in fetch of the lakes, position of the wind interface, and ongoing transition of incoming westerlies from Pacific westerlies to drier polar northwesterlies suggest that harsh winters continued (Fig. 4A and B).

Phase 2, ~12.9–11.5 ka

During P2, the GLEC was likely a southern boreal-type climate in summer but with a northern boreal-type winter. Changes between the subphases again can be linked to hydrologic changes, plus the position of the ice sheet and significant changes in the surface winds.

P2early, ~12.9–12.5 ka

The ARWs indicate that a southern boreal-type climate was established across the EOL-AP by the start of P2early, ~12.9 ka, concurrent with increasing lake surface area, the wind interface north of the Lake Ontario basin, and an overall reduction in meltwater flow south of the interface, including the absence of meltwater in ELE (Eschman and Karrow, 1985; Farrand and Drexler, 1985; Pair and Rodrigues, 1993; Webb et al., 2003; Rayburn et al., 2005, 2011; Anderson and Lewis 2012; Lewis et al., 2012; Watson et al., 2018; Leydet et al., 2018; Lewis and Todd, 2019; Fig. 3B). These conditions suggest increasing atmospheric temperatures and moisture content across the EOL-AP during P2early. However, the incoming westerlies had transitioned from cool Pacific westerlies to cold dry northwesterlies as the north-south corridor between the LIS and CIS widened (Dyke et al., 2003; Atkinson et al., 2016; Utting et al., 2016; Figs. 3B and C and 4B and C).

Outside the EOL-AP and HEOL, warmer conditions and different timelines of climate change are also suggested by spruce/pine pollen transitions in the southwestern AP and by pollen and the biomarkers of archaeal brGDGT (branched glycerol dialkyl glycerol tetraether membrane lipids) found in the lowlands west of the plateau (Shane, 1987; Shane and Anderson, 1993; Watson et al., 2018). However, the 12.9 ka onset of the YD cold interval is suggested at other interior lowland sites by pollen and brGDGT analyses (e.g., Gonzales and Grimm, 2009; Fastovich et al., 2020). These spatial differences suggest a changing boundary of the GLEC due to changes in the downwind side of the lakes and spatial extent of the GLEC over time.

By the end of P2early, ca 12.5 ka, the lake surface area south of the wind interface was at its maximum (Eschman and Karrow, 1985; Farrand and Drexler, 1985; Lowell et al., 1999, 2009; Dyke et al., 2003; Lewis et al., 2012; Lewis and Todd, 2019; Fig. 3C), and the interaction between lakes and northwesterlies may have been at its peak due to the maximum size of the lakes, configuration of the lakes and LIS, and the near-perfect arc of the southern LIS.

The southern boreal climate suggested by the ARWs coincides with the multiple open lakes preventing the cold northwesterlies from lowering summer temperatures in the EOL-AP and HEOL (Figs. 3B and C and 4B and C). However, frozen lakes had limited interaction with the winds, and the southern margin of the LIS may have increased the harshness of winter climate conditions.

P2mid, ~12.5–11.9 ka

A greater variation in climate with a more open environment is suggested by the sole representation of tamarack and higher ARWs, and it began with the opening of the North Bay–Ottawa River outlets of Lake Algonquin ca. 12.5 ka, which terminated any meltwater inflow into both ELE and Early Lake Ontario (ELO) and altered configuration and increased water temperatures of the lakes (Eschman and Karrow, 1985; Teller, 1987; Lowell et al., 1999; Dyke et al., 2003; Lewis et al., 2007, 2008; Anderson and Lewis, 2012; Hladyniuk and Longstaffe, 2016; Lewis and Anderson, 2017, 2019; Leydet et al., 2018; Figs. 3C and D and 4C and D).

The dominance of pioneer tamarack for more than 500 years also suggests disruptive environmental conditions, probably from higher variability in atmospheric temperatures and moisture content and/or greater frequency of climate extremes (e.g., Lowell et al., 1999; Dyke et al., 2003; Fig. 3C and D). The wind interface moved only slightly northward of the Trent River valley, which

https://doi.org/10.1017/qua.2021.76 Published online by Cambridge University Press

kept the EOL-AP within the band of northwesterlies (Schaetzl et al., 2016; Figs. 3C and 4C). The summer climate in the EOL-AP may have continued to be buffered by the increasing water temperatures of the lakes south of the wind interface, but harsh winters and perhaps more frequent seasonal freeze–thaw events continued across the EOL-AP.

P2late, ~11.9–11.7 ka

The natural progression of a pioneer ecosystem to at least a secondary forest is indicated by the return of spruce and ARWs at the same level as in P1early, suggesting a less disruptive environment with reduction in climate extremes and possible decrease in moisture levels during this phase. Water levels and lake surface area of the post–Lake Algonquin basins continued to decrease from the continuing drainage into the North Bay outlets and the Marquette Readvance (Teller, 1987; Lowell et al., 1999; Dyke et al., 2003; Lewis et al., 2008, 2012; Anderson and Lewis, 2012; Franzi et al., 2016; Fig. 3C and D). The wind interface moved to ~350 km north of the EOL-AP for the first time, which may have put the EOL-AP on the southern side of the band of strong northwesterlies, but the impact of the advancing Marquette Ice Lobe on the surface northwesterlies may have kept the EOL-AP well within that band (Filion, 1987; David, 1988; Dyke et al., 2003; Schaetzl et al., 2016; Figs. 3C and D and 4C and D). Harsh winters likely continued across the EOL-AP but may have started decreasing by the end of P2late.

P2final, ~11.7–11.5 ka

A continuation of drier and less variable climate is made evident by the development of the climax forest, as indicated by the increase in spruce and reduction in ARWs, but some retention of harsh winters is still suggested by the minimal thermophilous species. During P2final, the influence of the lakes on the polar northwesterlies continued to decline as lake size decreased and with the increasing distance between the ice sheet and EOL-AP (Figs. 3D and 4D). Both summer and winter climate conditions were improving as the wind interface moved north, and the EOL-AP was likely out of the range of the GLEC by the end of P2final.

Phase 3, ~11.5–10.5 ka

A mixed boreal and cool-temperate climate throughout the year, typical of the EH climate across northeastern North America, is suggested by the ARWs and species representation in P3. During this phase, all the lakes were at or fell to lowstands, remained isolated, and were no longer a major controlling factor in regional climate change (Lewis et al., 2007; Anderson and Lewis, 2012, Dyke et al., 2003, Lewis and Anderson, 2017; Figs. 3E and 4E).

Implications of tamarack and black ash

In general, the most reliable factors in addressing climate change in boreal environments are the pollen of spruce, pine, and nonarboreal species (e.g., Davis, 1963; Anderson, 1985; Jacobson et al., 1987; Webb et al., 2003). However, tamarack may have been a dominant species along with spruce throughout the LG interval. Changes in the percentage of spruce pollen may reflect changes in climate variables such as frequencies of extremes and/or fluctuations in moisture levels rather than changes in average temperatures. The use of tamarack can clarify the causal factors. The sole representation of black ash for thermophilous species, its species range and tolerance of cold temperatures supports the relatively warm summers in a northern boreal forest despite harsh winters in P1, and the warmer summers of a southern boreal climate with harsh winters prohibiting the establishment of other thermophilous species in P2, both of which confirm the seasonality suggested by the ARWs and other proxy records. Our interpretations suggest that hydrologic changes were recorded in the multiple data sets but in different ways over time and reflect the complexity of the changing Great Lakes system.

CONCLUSIONS

This study reveals that the climate anomaly in the EOL-AP was the result of a regional GLEC, created and maintained by the glacial Great Lakes and their interaction with the surface winds, LIS, and meltwater during the LG interval. Their effects on climate and timing of changes do not reflect the BA-YD-EH record of the Greenland ice core record and/or other proxy records outside the Great Lakes region and may explain inconsistencies in proxy records over time found within the Great Lakes region. These findings also suggest a regional lake-effect climate may exist wherever large lake(s) have significant impact on mesoscale atmospheric circulation and surface winds can transport those effects into the surrounding region.

The linkages of changes in the proxy records to changes in the Great Lakes system would have been limited without the tamarack. The equal representation of tamarack and spruce suggests that tamarack was a dominant species and its pioneer status and other growth characteristics resulted in a better evaluation of climate conditions and changes over time. The inclusion of black ash illustrates how particular thermophilous species may also be important climate proxies. The addition of tamarack to established climate reconstructions may significantly alter them but also contributes to our understanding of LG climate change, especially on a regional scale.

Overall, this study suggests that climate change in the southeastern Great Lakes region was significantly different and more complex than in the surrounding regions and adds a foundation for evaluating regional LG climate change.

Supplementary Material. The supplementary material for this article can be found at https://doi.org/10.1017/qua.2021.76

Acknowledgments. We thank Richard Laub and Norton Miller for sharing samples and the Ralph Bowering family and Robert Moffett for permission to excavate and collect material from their properties. We also thank the reviewers and Thomas Lowell for comments and extensive editing. Research was funded by the Eppley Foundation, Paleontological Research Institute, and National Geographic Society CRE no. 9725-15. This study is Contribution no. 20200704 of Natural Resources Canada. None of the authors have any competing interests.

Financial Support. Research was funded by the Eppley Foundation, Paleontological Research Institute, and National Geographic Society CRE no. 9725-15. None of the authors have any competing interests.

REFERENCES

Alley, R.B., 2000. The Younger Dryas cold interval as viewed from central Greenland. *Quaternary Science Reviews* **19**, 213–226.

Alley, R.B., 2004. GISP2 *Ice Core Temperature and Accumulation Data*. IGBP PAGES/World Data Center for Paleoclimatology, Data Contribution Series #2004-013. NOAA/NGDC Paleoclimatology Program, Boulder, CO.

Anderson, T.W., 1985. Late-Quaternary pollen records from Eastern Ontario, Quebec and Atlantic Canada. In: Bryant, V.M., Jr., Holloway, R.G. (Eds.), *Pollen Records of Late-Quaternary North American Sediments*. American Association of Stratigraphic Palynologists, Dallas, pp. 281–326.

Anderson, T.W., Lewis, C.F.M., 2012. A new water-level history for Lake Ontario basin: evidence for a climate-driven early Holocene lowstand. *Journal of Paleolimnology* **47**, 513–530.

Atkinson, N., Pawley, S., Utting, D.J., 2016. Flow-pattern evolution of the Laurentide and Cordilleran ice sheets across west-central Alberta, Canada: implications for ice sheet growth, retreat and dynamics during the last glacial cycle. *Journal of Quaternary Science* **31**, 753–768.

Bartlein, P.J., Prentice L.C., Webb, T., III, 1986. Climatic response surfaces from pollen data for some eastern North American taxa. *Journal of Biogeography* **13**, 35–57.

Berger, A.L., 1978. Long-term variations of caloric insolation resulting from the Earth's orbital elements. *Quaternary Research* **9**, 139–167.

Birks, H.H., 2003. The importance of plant macrofossils in the reconstruction of Lateglacial vegetation and climate: examples from Scotland, western Norway, and Minnesota, USA. *Quaternary Science Reviews* **22**, 453–473.

Blanken, P.D., Rouse, W.R., Schertzer, W.M., 2003. Enhancement of evaporation from a large northern lake by the entrainment of warm, dry air. *Journal of Hydrometeorology* **4**, 680–693.

Broecker, W.S., 2006. Was the Younger Dryas triggered by a flood? *Science* **312**, 1146–1148.

Bronk Ramsey, C., van der Plicht, J., Weninger, B., 2001. "Wiggle matching" radiocarbon dates. *Radiocarbon* **43**, 381–389.

Bryson, R.A., 1966. Air masses, streamlines and the boreal forest. *Geographical Bulletin* **8**, 228–269.

Burnett, A.W., Kirby M.E., Mullins H.T., Patterson W.P., 2003. Increasing Great Lake–effect snowfall during the twentieth century: a regional response to global warming? *Journal of Climate* **16**, 3535–3542.

Burns, R.M., Honkala, B.H. (Technical Coordinators), 1990. *Silvics of North America*. Vol. 1, *Conifers*; Vol. 2. *Hardwoods*. Agriculture Handbook 654. U.S. Department of Agriculture, Forest Service, Washington, DC.

Calkin, P.E., McAndrews, J.H., 1980. Geology and paleontology of two Late Wisconsin sites in western New York State. *Geological Society of America Bulletin* **91**, 295–306.

Coakley, J.P., Lewis, C.F.M., 1985. Postglacial lake levels in the Erie basin. In: Karrow, P.F., Calkin, P.E. (Eds.), *Quaternary Evolution of the Great Lakes*. Geological Association of Canada Special Publication 30. Geological Association of Canada, St. John's, NL, Canada, pp. 288–298.

Conroy, J.L., Karamperidou, C., Grimley, D.A., Guenthner, D.R., 2019. Surface winds across eastern and midcontinental North America during the Last Glacial Maximum: a new data-model assessment. *Quaternary Science Reviews* **220**, 14–29.

Cook, E.R., Kairiukstis, L.A. (Eds.), 1990. *Methods of Dendrochronology*. Kluwer Academic, Dordrecht, Netherlands.

Cordeira, J.M., Laird, N.F., 2008. The influence of ice cover on two lake-effect snow events over Lake Erie. *Monthly Weather Review* **136**, 2747–2763.

Dalton, A.S., Margold, M., Stokes, C.R., Tarasov, L., Dyke, A.S., Adams, R.S., Allard, S., *et al.*, 2020. An updated radiocarbon-based ice margin chronology for the last deglaciation of the North American Ice Sheet Complex. *Quaternary Science Reviews* **234**, 106–223.

David, P.P., 1988. The coeval eolian environment of the Champlain Sea episode. In: Gadd, N.R. (Ed.), *The Late Quaternary Development of the Champlain Sea Basin*. Geological Association of Canada Special Paper 35. Geological Association of Canada, St. John's, NL, Canada, pp. 291–305.

Davis, M.B., 1963. On the theory of pollen analysis. *American Journal of Science* **261**, 897–912.

Davis, M.B., 1969. Palynology and environmental history during the Quaternary period. *American Scientist* **57**, 317–332.

Desai, A.R., Austin, J.A., Bennington, V., McKinley, G.A., 2009. Stronger winds over a large lake in response to weakening air-to-lake temperature gradient. *Nature Geoscience* **2**, 855–858.

Dyke, A.S., 2004. An outline of North American deglaciation with emphasis on central and northern Canada. In: Ehlers, J., Gibbard, P.L. (Eds.), *Quaternary Glaciations—Extent and Chronology*. Part II. Elsevier, Amsterdam, pp. 373–424.

Dyke, A.S., 2005. Late Quaternary vegetation history of northern North America based on pollen, macrofossil, and faunal remains. *Géographie Physique et Quaternaire* **59**, 211–262.

Dyke, A.S., Moore, A., Robertson, L., 2003. *Deglaciation of North America*. Geological Survey of Canada, Open File 1574 (accessed September 15, 2019). https://doi.org/10.4095/214399.

Edwards, T.W.D., Aravena, R.O., Fritz, P., Morgan, A.V., 1985. Interpreting paleoclimate from ^{18}O and ^{2}H in plant cellulose: comparison with evidence from fossil insects and relict permafrost in southwestern Ontario. *Canadian Journal of Earth Science* **22**, 1720–1726.

Edwards, T.W.D., Wolfe, B.B., 1996. Influence of changing atmospheric circulation on precipitation $\delta^{18}O$–temperature relations in Canada during the Holocene. *Quaternary Research* **46**, 211–218.

Eschman, D.F., Karrow, P.F., 1985. Huron basin glacial lakes; a review. In: Karrow, P.F., Calkin, P.E. (Eds.), *Quaternary Evolution of the Great Lakes*. Geological Association of Canada Special Publication 30. Geological Association of Canada, St. John's, NL, Canada, pp. 79–93.

Farrand, W.R., Drexler, C.W., 1985. Late Wisconsinan and Holocene history of the Lake Superior basin. In: Karrow, P.F., Calkin, P.E. (Eds.), *Quaternary Evolution of the Great Lakes*. Geological Association of Canada Special Publication 30. Geological Association of Canada, St. John's, NL, Canada, pp. 17–32.

Fastovich, D., Russell, J.M., Jackson, S.T., Williams, J.W., 2020. Deglacial temperature controls on no-analog community establishment in the Great Lakes Region. *Quaternary Science Reviews* **234**, 106245.

Filion, L., 1987. Holocene development of parabolic dunes in the central St. Lawrence Lowland, Quebec. *Quaternary Research* **28**, 196–209.

Franzi, D.A., Ridge, J.C., Pair, D.L., Desimone, D., Rayburn, J.A., Barclay, D.J., 2016. Post-Valley Heads deglaciation of the Adirondack Mountains and adjacent lowlands. *Adirondack Journal of Environmental Studies* **21**, 119–146.

Fritz, P., Morgan, A.V., Eicher, U., McAndrews, J.H., 1987. Stable isotope, fossil Coleoptera and pollen stratigraphy in Late Quaternary sediments from Ontario and New York State. *Palaeogeography, Palaeoclimatology, Palaeoecology* **58**, 183–202.

Futyma, R.P., NG Miller, N.G., 2001. Postglacial history of a marl fen: vegetational stability at Byron-Bergen Swamp, New York. *Canadian Journal of Botany* **79**, 1425–1438.

Gonzales, L.M., Grimm, E.C., 2009. Synchronization of late-glacial vegetation changes at Crystal Lake, Illinois, USA with the North Atlantic Stratigraphy. *Quaternary Research* **72**, 234–245.

Griggs, C., Peteet, D., Kromer, B., Grote, T., Southon, J., 2017. A tree-ring and paleoclimate record for the Younger Dryas-Early Holocene transition from northeastern North America. *Journal of Quaternary Science* **32**, 341–346.

Griggs, C.B., Grote, T., 2016. The Younger Dryas to Early Holocene tree-ring radiocarbon, paleoecological and paleohydrological record for the Bell Creek Site, Lake Ontario Lowlands, New York State, USA. In: *Field Guidebook for 2016 Northeast Friends of the Pleistocene Meeting*. http://www2.newpaltz.edu/fop/pdf/FOP2016Guide.pdf, accessed 1 November 2018.

Griggs, C.B., Kromer, B., 2008. Wood macrofossils and dendrochronology of three mastodon sites in upstate New York. In: Allmon, W., Nester, P. (Eds.), *Mastodon Paleobiology, Taphonomy, and Paleoenvironment in the Late Pleistocene of New York State: Studies on the Hyde Park, Chemung, and Java Sites*. Palaeontographica Americana 61. Paleontological Research Institution, Ithaca, NY, pp. 49–61.

Harlow, W.M., 1959. *Fruit Key & Twig Key to Trees and Shrubs*. Dover Publications, New York.

Harlow, W.M., Harrar, E.S., White, F.M., 1979. *Textbook of Dendrology*. 6th ed. McGraw-Hill, New York.

Hegerl, G., Luterbacher, J., González-Rouco, F., Tett, F.B.S., Crowley, T., Xoplaki, E., 2011. Influence of human and natural forcing on European seasonal temperatures. *Nature Geosciences* **4**, 99–103.

Hladyniuk, R., Longstaffe, F.J., 2016. Paleoproductivity and organic matter sources in Late Quaternary Lake Ontario. *Palaeogeography, Palaeoclimatology, Palaeoecology* **435**, 13–23.

Hoadley, R.B., 1990. *Identifying Wood*. Taunton Press, Newtown, CT.

https://doi.org/10.1017/qua.2021.76 Published online by Cambridge University Press

Hostetler, S.W., Bartlein, P.J., Clark, P.U., Small, E.E., Solomon, A.M., 2000. Simulated influences of Lake Agassiz on the climate of central North America 11,000 years ago. *Nature* **405**, 334–337.

Jackson, S.T., Overpeck, J.T., Webb, T., III, Keattch, S.E., Anderson, K.H., 1997. Mapped plant-macrofossil and pollen records of late Quaternary vegetation change in Eastern North America. *Quaternary Science Reviews* **16**, 1–70.

Jacobson, G.L., Jr., Webb, T., III, Grimm, E.C., 1987. Patterns and rates of vegetation change during the deglaciation of eastern North America In: Ruddiman, W.F., Wright, H.E., Jr. (Eds.), *North America and Adjacent Oceans during the Last Deglaciation*. The Geology of North America, Vol. K-3. Geological Society of America, Boulder, CO, pp. 277–288.

Jarvis, P., Linder, S., 2000. Constraints to growth of boreal forests. *Nature* **405**, 904–905.

Kaiser, K.F., 1994. Two Creeks interstade dated through dendrochronology and AMS. *Quaternary Research* **42**, 288–298.

Karrow, P.F., Warner, B.G., 1988. Ice, lakes, and plants, 13,000 to 10,000 years BP: the Erie-Ontario lobe in Ontario. In: Laub, R.S., Miller, N.G., Steadman, D.W. (Eds.), *Late Pleistocene and Holocene Paleoecology and Archaeology of the Eastern Great Lakes Region*. Proceedings of the Smith Symposium, Buffalo Museum of Science, October 24–25, 1986. *Bulletin of the Buffalo Society of Natural Sciences* 33, 39–52.

Kreyling, J., Schmid, S., Aas, G., 2015. Cold tolerance of tree species is related to the climate of their native ranges. *Journal of Biogeography* **42**, 156–166.

Kristovich, D.A.R., Laird, N.F., 1998. Observations of widespread lake-effect cloudiness: influences of lake surface temperature and upwind conditions. *Weather and Forecasting* **13**, 811–821.

Laird, N.F., DesRochers, J., Payer, M., 2009. Climatology of lake-effect precipitation events over Lake Champlain. *Journal of Applied Meteorology and Climatology* **48**, 232–251.

Laird, N.F., Walsh, J.E., Kristovich, D.A.R., 2003. Model simulations examining the relationship of lake-effect morphology to lake shape, wind direction, and wind speed. *Monthly Weather Review* **131**, 2102–2111.

Lang, C.E., McDonald, J.M., Gaudet, L., Doeblin, D., Jones, E.A., Laird, N.F., 2018. The influence of a lake-to-lake connection from Lake Huron on the lake-effect snowfall in the vicinity of Lake Ontario. *Journal of Applied Meteorology and Climatology* **57**, 1423–1439.

Laub, R.S., 2003a. The Hiscock site: structure, stratigraphy and chronology. In: *The Hiscock Site: Late Pleistocene and Holocene Paleoecology and Archaeology in Western New York State*. Proceedings of the Second Smith Symposium, Buffalo Museum of Science, October 14–15, 2001. *Bulletin of the Buffalo Society of Natural S*ciences 37, 18–38.

Laub, R.S. (Ed.), 2003b. *The Hiscock Site: Late Pleistocene and Holocene Paleoecology and Archaeology in Western New York State*. Proceedings of the Second Smith Symposium, Buffalo Museum of Science, October 14–15, 2001. Bulletin of the Buffalo Society of Natural Sciences 37.

Laub, R.S., McAndrews, J.H., 1999. Beaver (*Castor canadensis*) and mastodon (*Mammut americanum*) in a Late-Pleistocene upland spruce forest, western New York State. *Current Research in the Pleistocene* **16**, 139–140. Erratum in 2000 CRP 17:153.

Laub, R.S., McAndrews, J.H., 2000. Erratum to: Beaver (*Castor canadensis*) and mastodon (*Mammut americanum*) in a Late-Pleistocene upland spruce forest, western New York State. *Current Research in the Pleistocene* **17**, 153.

Laub, R.S., Miller, N.G., Steadman, D.W. (Eds.), 1988. *Late Pleistocene and Holocene Paleoecology and Archaeology of the Eastern Great Lakes Region*. Proceedings of the Smith Symposium, Buffalo Museum of Science, October 24–25, 1986. *Bulletin of the Buffalo Society of Natural Sciences* 33.

Lewis, C.F.M., Anderson, T.W., 2017. Sediment sequences and palynology of outer South Bay, Manitoulin Island, Ontario: connections to Lake Huron paleohydrologic phases and upstream Lake Agassiz events. *Quaternary Science Reviews* **173**, 248–261.

Lewis, C.F.M., Anderson, T.W., 2019. A younger glacial Lake Iroquois in the Lake Ontario basin, Ontario and New York: re-examination of pollen stratigraphy and radiocarbon dating. *Canadian Journal of Earth Sciences* **57**, 453–463.

Lewis, C.F.M., Cameron, G.D.M., Anderson, T.W., Heil, C.W., Jr., Gareau, P.L., 2012. Lake levels in the Erie basin of the Laurentian Great Lakes. *Journal of Paleolimnology* **47**, 493–511.

Lewis, C.F.M., Heil, C.W., Jr., Hubeny, J.B., King, J.W., Moore, T.C., Jr., Rea, D.K., 2007. The Stanley unconformity in Lake Huron basin: evidence for a climate-driven closed lowstand about 7900 ^{14}C BP with similar implications for the Chippewa lowstand in Lake Michigan basin. *Journal of Paleolimnology* **37**, 435–452.

Lewis, C.F.M., King, J.W., Blasco, S.M., Brooks, G.R., Coakley, J.P., Crowley, T.E., Dettman, D.L., *et al.*, 2008. Dry climate disconnected the Laurentian Great Lakes. *EOS Transactions, American Geophysical Union* **89**, 541–542.

Lewis, C.F.M., Todd, B.J., 2019. The Early Lake Ontario barrier beach: evidence for sea level about 12.8–12.5 cal. ka BP beneath western Lake Ontario in eastern North America. *Boreas* **48**, 195–214.

Leydet, D.J., Carlson, A.E., Teller, J.T., Breckenridge, A., Barth, A.M., Ullman, D.J., Sinclair, G., Milne, G.A., Cuzzone, J.K., Caffee, M.W., 2018. Opening of glacial Lake Agassiz's eastern outlets by the start of the Younger Dryas cold period. *Geology* **46**, 155–158.

Libicki, C., Bedford, K.W., 1990. Sudden, extreme Lake Erie storm surges and the interaction of wind stress, resonance, and geometry. *Journal of Great Lakes Research* **16**, 380–395.

Long, Z., Perrie, W., Gyakum, J., Caya, D., Laprise, R., 2007. Northern lake impacts on local seasonal climate. *Journal of Hydrometeorology* **8**, 881–896.

Lowell, T., Larson, G.H., Hughes, J.D., Denton, G.H., 1999. Age verification of the Lake Gribben forest bed and the Younger Dryas Advance of the Laurentide Ice Sheet. *Canadian Journal of Earth Science* **36**, 383–393.

Lowell, T.V., Fisher, T.G., Hajdasc, I., Glover, K., Loopee, H., Henry, T., 2009. Radiocarbon deglaciation chronology of the Thunder Bay, Ontario area and implications for ice sheet retreat patterns. *Quaternary Science Reviews* **28**, 1597–1607.

Mann, G.E., Wagenmaker, R.E., Sousounis, P.J., 2002. The influence of multiple lake interactions upon lake-effect storms. *Monthly Weather Review* **130**, 1510–1530.

Mielko, C., Woo, M.-K., 2006. Snowmelt runoff processes in a headwater lake and its catchment, subarctic Canadian Shield. *Hydrological Processes* **20**, 987–1000.

Miller, D., Gingerich, J., 2013. Regional variation in the terminal Pleistocene and early Holocene radiocarbon record of eastern North America. *Quaternary Research* **79**, 175–188.

Miller, N.G., 1973. *Late-glacial and Postglacial Vegetation Change in Southwestern New York State*. New York State Museum and Science Service, Bulletin 420. University of the State of New York, State Education Department, Albany.

Miller, N.G., 1988. The Late Quaternary Hiscock site, Genesee County, New York: paleontological studies based on pollen and plant macrofossils. In: Laub, R.S., Miller, N.G., Steadman, D.W. (Eds.), *Late Pleistocene and Early Holocene Paleoecology and Archaeology of the Eastern Great Lakes Region*. Proceedings of the Smith Symposium, Buffalo Museum of Science, October 24–25, 1986. *Bulletin of the Buffalo Society of Natural Sciences* 33, 83–93.

Miller, N.G., Futyma, R.P., 2003. Extending the paleobotanical record at the Hiscock site, New York: correlations among stratigraphic pollen assemblages from nearby lake and wetland basins. In: Laub, R.S. (Ed.), *The Hiscock Site: Late Pleistocene and Early Holocene Paleoecology and Archaeology of Western New York State*. Proceedings of the Second Smith Symposium, Buffalo Museum of Science, October 14–15, 2001. *Bulletin of the Buffalo Society of Natural Sciences* 37, 43–62.

Miller, N.G., Griggs, C.B., 2012. Tree macrofossils of Younger Dryas age from Cohoes, New York State, USA. *Canadian Journal of Earth Sciences* **49**, 671–680.

Miller, R.F., Morgan, A.V., 1981. A postglacial Coleopterous assemblage from Lockport Gulf, New York. *Quaternary Research* **17**, 258–274.

Morgan, A.V., 1972. Late Wisconsinan ice-wedge polygons near Kitchener, Ontario, Canada. *Canadian Journal of Earth Sciences/Revue Canadienne des Sciences de la Terre* **9**, 607–617.

Mott, R.J., Farley-Gill, L.D., 1978. A Late-Quaternary pollen profile from Woodstock, Ontario. *Canadian Journal of Earth Sciences* **15**, 1101–1111.

Motz, J.E., Morgan, A.V., 2001. Holocene paleoclimate and paleoecology determined from fossil Coleoptera at Brampton, Ontario, Canada. *Canadian Journal of Earth Sciences* **38**, 1451–1462.

Muschitiello, F., Wohlfarth, B., 2015. Time-transgressive environmental shifts across Northern Europe at the onset of the Younger Dryas. *Quaternary Science Reviews* **109**, 49–56.

https://doi.org/10.1017/qua.2021.76 Published online by Cambridge University Press

Pair, D.L., Rodrigues, C.G., 1993. Late Quaternary deglaciation of the southwestern St. Lawrence Lowland, New York and Ontario. *Geological Society of America Bulletin* **105**, 1151–1164.

Passerelli, R.E., Jr., Braham, R.R., Jr., 1981. The role of the winter land breeze in the formation of Great Lake snow storms. *Bulletin American Meteorological Society* **62**, 482–491.

Peteet, D., 1995. Global Younger Dryas? *Quaternary International* **28**, 93–104.

Pisaric, M.F.J., MacDonald, G.M., Velichko, A.A., Cwynar, L.C., 2001. The lateglacial and postglacial vegetation history of the northwestern limits of Beringia, based on pollen, stomate and tree stump evidence. *Quaternary Science Reviews* **20**, 235–245.

Rayburn, J., Knuepfer, P., Franzi, D., 2005. A series of large, Late Wisconsinan meltwater floods through the Champlain and Hudson Valleys, New York State, USA. *Quaternary Science Reviews* **24**, 2410–2419.

Rayburn, J.A., Cronin, T.M., Franzi, D.A., Knuepfer, P.L.K., Willard, D.A., 2011. Timing and duration of North American glacial lake discharges and the Younger Dryas climate reversal. *Quaternary Research* **75**, 541–551.

Reimer, P.J., Austin, W.E., Bard, E., Bayliss, A., Blackwell, P.G., Bronk Ramsey, C., Butzin, M., *et al.*, 2020. The IntCal20 Northern Hemisphere Radiocarbon Age Calibration Curve (0–55 cal kBP). *Radiocarbon* **62**, 725–757.

Renssen, H., 2020. Comparison of climate model simulations of the Younger Dryas cold event. *Quaternary* **3**, 29.

Renssen, H., Goosse, H., Roche, D.M., Seppä, H., 2018. The global hydroclimate response during the Younger Dryas event. *Quaternary Science Reviews* **193**, 84–97.

Rind, D., 1987. Components of the ice age circulation, *Journal of Geophysical Research*, **92**, 4241–4281.

Rouse, W.R., Blyth, E.M., Crawford, R.W., Gyakum, J.R., Janowicz, J.R., Kochtubajda, B., Leighton, H.G., *et al.*, 2003. Energy and water cycles in a high-latitude, north-flowing river system: summary of results from the Mackenzie GEWEX Study—Phase 1. *Bulletin of the American Meteorological Society* **8**, 73–87.

Saarnisto, M., 1974. The deglaciation history of the Lake Superior region and its climatic implications. *Quaternary Research* **4**, 316–339.

Samuelsson, P., Tjernström, M., 2001. Mesoscale flow modification induced by land/lake surface temperature and roughness differences. *Journal of Geophysical Research* **106**, 12419–12435.

Schaetzl, R.J., Krist, F.J., Lewis, C.F.M., Luehmann, M.D., Michalek, M.J., 2016. Spits formed in Glacial Lake Algonquin indicate strong easterly winds over the Laurentian Great Lakes during late Pleistocene. *Journal of Paleolimnology* **55**, 49–65.

Schaetzl, R.J., Yansa, C.H., Luehmann, M.D., 2013. Paleobotanical and environmental implications of a buried forest bed in northern Lower Michigan, USA. *Canadian Journal of Earth Science* **50**, 483–493.

Schweingruber, F.H., 1990. *Anatomie europäischer Hölzer/Anatomy of European Woods*. Swiss Federal Institute for Forest, Snow, and Landscape Research, Birmensdorf; Paul Haupt, Berne.

Scott, R.W., Huff, F.A., 1996. Impacts of the Great Lakes on regional climate conditions. *Journal of Great Lakes Research* **22**, 845–863.

Shane, L.C.K., 1987. Late-glacial vegetational and climate history of the Allegheny Plateau and the Till Plains of Ohio and Indiana, USA. *Boreas* **16**, 1–20.

Shane, L.C.K., Anderson, K.H., 1993. Intensity, gradients and reversals in late glacial environmental change in east-central North America. *Quaternary Science Reviews* **12**, 307–320.

Shuman, B., Webb, T., III, Bartlein, P., Williams, J.W., 2002. The anatomy of a climatic oscillation: vegetation change in eastern North America during the Younger Dryas chronozone. *Quaternary Science Reviews* **21**, 1777–1791.

Solanki, S.K., Usoskin, I.G., Kromer. B., Schüssler, M., Beer, J., 2004. An unusually active sun during recent decades compared to the previous 11,000 years. *Nature* **431**, 1084–1087.

Sousounis, P.J., Fritsch, J.M., 1994. Lake-aggregate mesoscale disturbances. Part II: A case study of the effects on synoptic-scale weather. *Bulletin of the American Meteorological Society* **75**, 1793–1811.

Spear, R.W., Davis, M.B., Shane, L.C.K., 1994. Late Quaternary history of low- and mid-elevation vegetation in the White Mountains of New Hampshire. *Ecological Monographs* **64**, 85–109.

Sperry, J.S., Nichols, K.L., Sullivan, J.E.M., Eastlack, S.E., 1994. Xylem embolism in ring-porous, diffuse-porous, and coniferous trees of Northern Utah and Interior Alaska. *Ecology* **75**, 1736–1752.

Strimbeck, G.R., Schaberg, P.G., Fossdal, C.G., Schröder, W.P., Kjellsen, T.D., 2015. Extreme low temperature tolerance in woody plants. *Frontiers in Plant Science* **6**, 884.

Sutton, R.F., 1969. *Silvics of white spruce (Picea glauca (Moench) Voss)*. Canadian Forestry Branch Publication 1250. Department of Fish and Forestry, Ottawa.

Teller, J.T., 1987. Proglacial lakes and the southern margin of the Laurentide Ice sheet. In: Ruddiman, W.F., Wright, H.E., Jr. (Eds.), *North America and Adjacent Oceans during the Last Deglaciation*. The Geology of North America, Vol. K-3. Geological Society of America, Boulder, CO, pp. 39–70.

Tinkler, K.J., Pengelly, J.W., 1994. Protalus ramparts and related features along the Niagara Escarpment, Niagara Peninsula, Ontario. *Permafrost and Periglacial Processes* **5**, 171–184.

Tinkler, K.J., Pengelly, J.W., Parkins, W.G., Terasmae, J., 1992. Evidence for high water levels in the Erie basin during the Younger Dryas Chronozone. *Journal of Paleolimnology* **7**, 215–234.

Ullman, D.J., LeGrande, A.N., Carlson, A.E., Anslow, F.S., Licciardi, J.M., 2014. Assessing the impact of Laurentide Ice Sheet topography on glacial climate. *Climate of the Past* **10**, 487–507.

Utting, D.J., Atkinson, N., Pawley, S., Livingstone, S.J., 2016. Reconstructing the confluence zone between Laurentide and Cordilleran ice sheets along the Rocky Mountain Foothills, south-west Alberta. *Journal of Quaternary Science* **31**, 769–787.

Vaganov, E.A., Hughes, M.K., Kirdyanov, A.V., Schweingruber, F.H., Silkin, P.P., 1999. Influence of snowfall and melt timing on tree growth in subarctic Eurasia. *Nature* **400**, 149–151.

Vavrus, S., Notaro, M., Zarrin, A., 2012. The role of ice cover in heavy lake-effect snowstorms over the Great Lakes basin as simulated by RegCM4. *Monthly Weather Review* **141**, 148–165.

Veels, P.C., Steenburgh, W.J., 2015. Climatological characteristics and orographic enhancement of lake-effect precipitation east of Lake Ontario and over the Tug Hill Plateau. *Monthly Weather Review* **143**, 3591–3609.

Villani, J.P., Jurewicz, M.L., Sr., Reinhold, K., 2017. Forecasting the inland extent of lake effect snow bands downwind of Lake Ontario. *Journal of Operational Meteorology* **5**, 53–70.

Watson, B.I., Williams, J.W., Russell, J.M., Jackson, S.T., Shane, L., Lowell, T.V., 2018. Temperature variations in the southern Great Lakes during the last deglaciation: comparison between pollen and GDGT proxies. *Quaternary Science Reviews* **182**, 78–92.

Webb, T., III, Laseski, R.A., Bernabo, J.C., 1978. Sensing vegetational patterns with pollen data: choosing the data. *Ecology* **59**, 1151–1163.

Webb, T., III, Shuman, B., Leduc, P., Newby, P., Miller, N., 2003. Late Quaternary climate history of western New York State. In: Laub, R.S. (Ed.), *The Hiscock Site: Late Pleistocene and Early Holocene Paleoecology and Archaeology of Western New York State*. Proceedings of the Second Smith Symposium, Buffalo Museum of Science, October 14–15, 2001. *Bulletin of the Buffalo Society of Natural Sciences* 37, 11–17.

Weiss, C.C., Sousounis, P.J., 1999. A climatology of collective lake disturbances. *Monthly Weather Review* **127**, 565–574.

Williams, J.W., Shuman, B., 2008. Obtaining accurate and precise environmental reconstructions from the modern analog technique and North American surface pollen dataset. *Quaternary Science Reviews* **27**, 669–687.

Wright, D.M., Posselt, D.J., Steiner, A.L., 2012. Sensitivity of lake-effect snowfall to lake ice cover and temperature in the Great Lakes region. *Monthly Weather Review* **141**, 670–689.

Young, R.A., Gordon, L.M., Owen, L.A., Huot, S., Zerfas, T.D., 2020. Evidence for a late glacial advance near the beginning of the Younger Dryas in western New York State: an event postdating the record for local Laurentide ice sheet recession. *Geosphere* **17**, 271–305.

Yu, Z., 2000. Ecosystem response to Lateglacial and Early Holocene climate oscillations in the Great Lakes region of North America. *Quaternary Science Reviews* **19**, 1723–1747.

Yu, Z., Wright, H.E., Jr., 2001. Response of interior North America to abrupt climate oscillations in the North Atlantic region during the last deglaciation. *Earth-Science Reviews* **52**:333–369.

https://doi.org/10.1017/qua.2021.76 Published online by Cambridge University Press